



Project Number: 774571  
Start Date of Project: 2017/11/01  
Duration: 48 months



## **Type of document 5.1 – V1.0**

## **Water Management Control**

Dissemination level	PU
Submission Date	2018-08-31
Work Package	WP5
Task	T5:3
Type	Report
Version	1.0
Authors	Nicolás Bono Rosselló, Andrea Gasparri and Emanuele Garone
Approved by	Andrea Gasparri + PMC

### **DISCLAIMER:**

The sole responsibility for the content of this deliverable lies with the authors. It does not necessarily reflect the opinion of the European Union. Neither the REA nor the European Commission are responsible for any use that may be made of the information contained therein.

---

## Executive Summary

This document aims at proposing a model and control methodology for irrigation systems in large-scale hazelnut orchards. First, we provide an analysis of current best practices in hazelnut orchards. Successively, we derive a dynamical model for the irrigation of large-scale hazelnut orchard. Then, we present novel control solutions to improve current irrigation management systems. Briefly, the main contributions of this deliverables are as follows:

1. State of the art analysis: Identification of current techniques for irrigation.
2. System modelling: Study and definition of a water balance model for soil and plant.
3. Control design: Definition of control techniques to perform irrigation control.
4. Numerical validation: Simulations to numerically validate the effectiveness of the proposed control strategies.

**Table of Content**

1	Introduction .....	6
2	Modelling of the system .....	8
2.1	Overall Description of the modelling philosophy .....	8
2.2	Soil dynamics .....	8
2.2.1	Geometric Characterization of the soil.....	8
2.2.2	Soil water storage model.....	9
2.2.3	Evapotranspiration .....	10
2.2.4	Irrigation .....	12
2.2.5	Rainfall .....	12
2.2.6	Surface runoff.....	12
2.2.7	Deep percolation .....	13
2.2.8	Underground runoff .....	13
2.2.9	Capillary rise.....	14
2.2.10	Soil moisture dynamics.....	14
2.3	Water plant storage model.....	15
2.4	Overall Model .....	18
2.4.1	Overall Model: Including actuation .....	20
2.4.2	Overall Model: Including sensing .....	20
2.4.3	Overall Model - Equations .....	21
2.4.4	Overall Model: The single soil parcel - single plant model .....	22
3	Control Techniques for Irrigation .....	23
3.1	Single Soil Parcel - Single Plant Water Storage Model .....	23
3.1.1	Model Parameter Selection and Evapotranspiration Data .....	23
3.1.2	Proportional Controller based on Leaf Measurements .....	26
3.1.3	Proportional Controller based on Leaf Measurements and Soil Moisture Measurements.....	29
3.1.4	Observer-based Control Design based on Leaf Measurements.....	33
3.1.5	Performances Comparison.....	41
3.2	Controlling the Entire Orchard.....	42

---

3.2.1	Insights from the Control of the Single Soil Parcel - Single Plant Water Storage and Preliminary Discussion .....	42
3.2.2	Observers .....	42
3.2.3	Control of the entire orchard .....	44
4	Validation of the model .....	46
4.1	High detail soil mapping experimental plots .....	46
4.2	Leaf water test .....	47

---

## Abbreviations and Acronyms

FAO	Food and Agriculture Organization of the United Nations
ET <sub>o</sub>	Reference evapotranspiration
I	Irrigation
UG	Underground runoff
C	Capillary rise
R	Rainfall
P	Deep percolation
SR	Surface runoff
MPC	Model predictive control
NVDI	Normalized vegetation index
FEM	Finite-Element Method

## 1 Introduction

The need for better water management systems is pushing agronomists and farmers to develop and use new irrigation techniques and policies. Accordingly, several control techniques have been introduced in the literature for the precision farming in the context of fields irrigation, see [1] for a comprehensive overview.

However, to the best of our knowledge, existing advanced techniques fall short of providing efficient and realistically implementable solutions for orchards. The main limit of most of the techniques surveyed in [1] is their assumptions in terms of sensing. For instance, most of them assume the possibility to perform direct measurements (e.g. with moisture sensors) on each plant, which is not realistic in a large-scale orchard.

The goal of this deliverable is to present the preliminary analysis and results developed in the project PANTHEON for modelling and control of the irrigation of large-scale hazelnut plantations. These results represent the theoretical guideline that will drive tests and validation activities to be performed on the field.

To the best of our knowledge, this deliverable represents the first attempt ever regarding precision farming in terms of irrigation control for hazelnut plantations. Indeed, in current best practices, the irrigation of a hazelnut orchard is usually carried out through fixed equipment and may consist mainly of drippers, or sprinklers, or sometimes a mix of both. Typically, for plantations bigger than 50 ha, water treatment is the same for homogeneous portions of 5-10 ha (up to 50 ha in very large plantations). Water levels are usually regulated through remotely controlled valves. Nowadays, irrigation levels are usually decided by the agronomist or the farmer based on a qualitative evaluation and on quite scarcely sampled quantitative measurements (mostly direct observation). Current best practices may have a relevant negative impact on the environmental sustainability and economic cost of the orchard, as the very coarse granularity and the subjectivity and arbitrariness of the valves opening may easily result in an “over-irrigation” (with consequent waste of water) or in “under-irrigation” (with consequent water stress of the plants and loss of productivity).

We believe that, using the architecture proposed in the PANTHEON project, and coupling it with an in-depth agronomical knowledge of hazelnuts and with the tools of systems and control theory, it is possible to achieve a relevant improvement with respect to the current best practice.

It is worth to mention that what we propose in this deliverable is not a mere extension of what done for other kinds of crops. Indeed most of existing techniques are usually based on a single kind of measurement/estimation of certain variables, e.g. certain techniques are uniquely based on soil moisture [2]–[4] other focus on the plant status [5]–[7], etc.

Following a system theoretic approach, we propose to go beyond “focusing on few aspects”. In this regard, the underlying idea is to consider the orchards as a dynamic system whose state includes both the soil moisture and the content of water in the plants, and where interactions between soil, plants, and weather are considered. On the basis of this model, and on the characterization of the sensing capabilities (type of sensors and their placement) and of the available actuation (irrigation valves), we propose a simple and yet scalable control strategy for the irrigation control of large-scale hazelnut plantations.

The remainder of this deliverable is organized as follows.

In Section 2 we will describe in depth the modelling of the orchard and of all its subparts, included the parameters, their meaning, and possible way to identify the actual parameters when data will be available. This section will also include a discussion on how to include in the model the available sensing and actuation.

In Section 3 we will focus on the simple case of “an orchard of 1 tree”. This case is very informative to show the limits of simple static feedback control laws, and advocate for the use of a state-space based approach



---

consisting of state-observers and state-feedbacks. Furthermore, a scalable control architecture for the entire hazelnut orchards is discussed.

In Section 4 a discussion concerning future work directions for the experimental validation of the proposed modelling is provided.

## 2 Modelling of the system

### 2.1 Overall Description of the modelling philosophy

In this deliverable, we consider the “orchard system” as a collection of trees and of soil plots (or parcels) that interact with each other exchanging water.

Using the existing literature, and filling the gaps we will develop a model describing:

- How the water is absorbed and stored in the soil.
- How the plants use this water during the day.
- How external disturbances (solar radiation, air temperature, humidity and rain) and controlled inputs (irrigation) enter in these dynamics

Once this descriptive model is completed, we will extend it considering the dynamics and the characteristics of the sensors and the specific geometry of the actuators we plan to use in our setting.

### 2.2 Soil dynamics

#### 2.2.1 Geometric Characterization of the soil

In line of principle the soil should be considered as a continuous dynamical system in 3 dimensions (included depth up to some meters) and described by Partial Differential Equations. Clearly this would result in a model that is not easily treatable, and even more hardly identifiable.

To build a dynamical model of the soil that is tractable, and yet informative enough to build an irrigation control architecture, we consider a Finite Element Method Like (FEM) approximation of the soil. In particular we will

- Following the example of [8], we consider the soil as composed of a single layer. In first approximation this is very reasonable as most of the trees’ roots are concentrated at a specific depth around 40-50 cm underground
- We divide the field in small rectangular plots (nodes) and we consider it as a single variable, i.e. for each node  $i$ , we will consider the evolution of one variable  $\theta_i$  that we will denote as **soil moisture** representing the quantity of water in the  $i$ -th note.

As a result, what we obtain is a representation of the field as a collection of nodes, as depicted in Figure 1.

Clearly, nodes interact with each other. In particular, it is reasonable to assume that each node interacts directly only with its neighbours (to show what we mean by neighbours in Figure 2 a dark blue parcel node is depicted together with its neighbouring nodes coloured in light blue). Each node  $i$  is identified by its centroid  $v_i$  (uniquely described by its geographical coordinates). The fact that two nodes  $i$  and  $j$  are neighbours is naturally represented through the existence of an edge  $(v_i, v_j)$  between them. Using standard graph theory [9] we can then describe the interconnection between nodes by means of a graph  $G = \{V, E\}$  with the set of nodes  $V = \{v_1, \dots, v_n\}$  and the set of edges  $E = \{(v_i, v_j)\}$  denotes neighbourhood relations.

Note that, for the sake of model generality the parcel size at the current stage is not fixed.

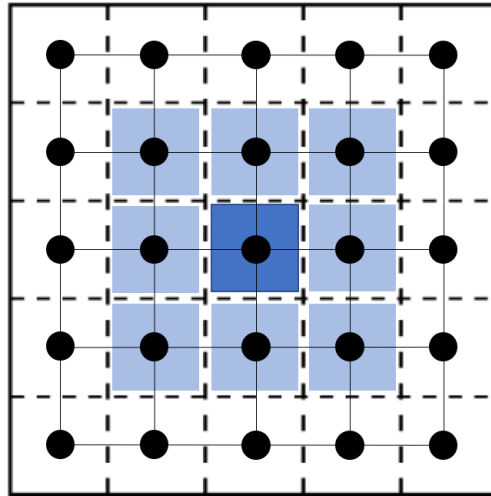


Figure 1: Division of the field into squares

### 2.2.2 Soil water storage model

In our setting, we are going to define the process dynamics of the soil nodes by resorting to a hydrological balance model. A common approach to derive a soil water storage model, that can be found in [3]–[5] and [12], is to consider the soil water storage variation  $\Delta S$  as the result of the soil water inflows  $S_{in}$  (irrigation, rainfall, capillary rise and horizontal ground inflow) minus the soil water outflows  $S_{out}$  (evapotranspiration, deep percolation, and horizontal water outflow), so as:

$$\Delta S = S_{in} - S_{out} \quad (1)$$

By denoting with  $\dot{\theta}_i$  the **soil moisture variation** at node  $i$ , that is the variation on the amount of water stored at node  $i$ , we obtain the following differential equation for each node  $i$ :

$$\dot{\theta}_i = -ET_i + I_i + R_i \pm SR_i - P_i + UG_i + C_i \quad (2)$$

where each parameter has the following meaning:

- $ET_i$  is called **evapotranspiration** and can be defined as the sum of the water extracted from the soil through evaporation in the surface of the node  $i$  and the water absorption due the plant drawing from that parcel.
- $I_i$  is called **irrigation** and is the water provided to the node  $i$  by the irrigation system.
- $R_i$  is called **precipitation** and it corresponds to the amount of water provide to the node  $i$  by the rainfall.
- $SR_i$  is called **surface runoff** and can be defined as the quantity of water runoff from the surface of the node  $i$ .
- $P_i$  is called **deep percolation** and can be defined as the water moved downwards to a deeper level of soil.
- $UG_i$  is called **underground flow** and represents the movement of water between different parcels.
- $C_i$  is called **capillary rise** and is the amount of water absorbed by the root zone from a deeper layer of soil.

Figure 1 provides a graphical representation of the meaning of all the terms involved in the soil water storage dynamical model derivation.

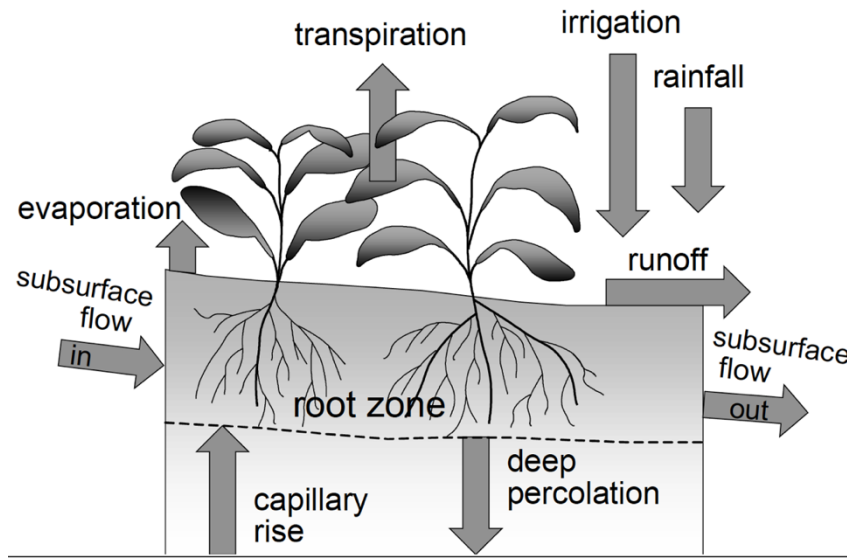


Figure 1 - Soil water storage dynamical model

Compared to the works at the state of the art, the major novelty introduced by our formulation is that we are not considering a homogenous soil moisture status for the whole orchard, but rather we are introducing a finite-element representation of the soil to better describe the heterogenous characteristics of the orchard in different areas of the field. In the sequel, a detailed description of the different parameters which are involved in the modelling of the soil moisture balancing equation is given. Note that in the sequel the subscript  $i$  denoting the parcel  $i$  to which the parameter is referred to will be omitted if not strictly required, for the sake of readability.

### 2.2.3 Evapotranspiration

A recurrent term in irrigation literature is **evapotranspiration** denoted as  $Et$ , where the amount of water extracted from the soil by **plant transpiration** and **soil evaporation** are combined [10]. The reason why the term evapotranspiration is so popular is due to the fact that it can be easily computed using the information provided by a meteorological station, while it is experimentally not straightforward to compute the two terms separately.

A popular modelling of evapotranspiration can be found in [10], where the reference evapotranspiration  $ET_0$  is calculated using the Penman–Monteith equation for specific reference conditions [11] and a coefficient  $K_c$  adapts its value to the kind of crop and its phenological phases. Accordingly, the following equation describes the reference evapotranspiration  $ET_0$ :

$$ET_0 = \frac{0.4081\Delta(Rn - G)\gamma \frac{900}{T_a + 273} u_2 (e_s - e_a)}{\Delta + \gamma(1 + 0.34 * u_2)} \quad (3)$$

while the evapotranspiration  $ET_c$  can be computed accordingly as:

$$ET_c = K_c * ET_0. \quad (4)$$

Note that all the parameters can be obtained from the weather conditions using a meteorological weather station. To the best of our knowledge, apart from [12], not many studies can be found for the computation

of  $K_c$  coefficients regarding hazelnut crops. Furthermore, it should be noticed that according to the current state of the art, the evapotranspiration  $ET_c$  is applied homogenously to the whole field.

In order to provide accurate information about the crop status, inspired by [4], within the PANTHEON project we plan to compute the evapotranspiration coefficient  $K_c$  by resorting to the NDVI (Normalized Difference Vegetation Index) index. Briefly, NDVI is a measurement available from remote sensing that quantifies the green vegetation index by measuring the difference between near-infrared (which vegetation strongly reflects) and red light (which vegetation absorbs). More specifically, in [4],  $ET_c$  values from maize orchards were calculated using the NDVI coefficient according to the following equation:

$$K_c = 1.15 * NDVI + 0.17 \tag{5}$$

Briefly, the relationship presented in eq. (5) was obtain in [4] by resorting to system identification techniques. Always in [4], this relationship was later tested on the experimental field were, according to Figure 2, actual crop water requirements were similar to the ones obtained by means of eq. (5) through remote sensing data, whereas they were 20% less than those obtained from the FAO methodology. In our case, in order to obtain a similar insight of the use of NDVI, once a relation between  $K_c$  and NDVI is obtain for the hazelnut crop, we plan to compare their behaviour with the  $K_c$  parameters computed in [12].

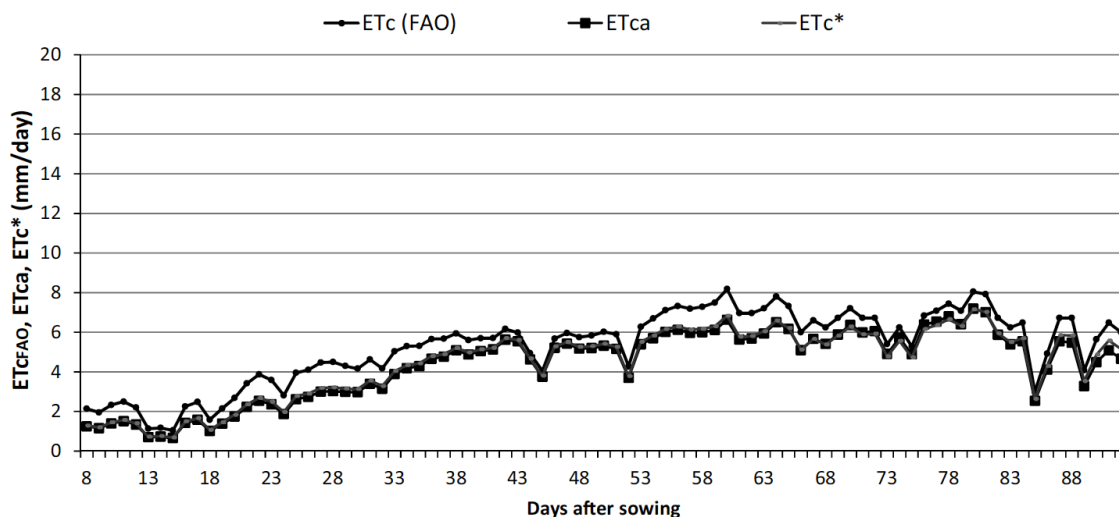


**Figure 2:** Crop evapotranspiration determined by 3 different  $K_c$  factors: in situ determinations of actual  $K_c$  (ETca), FAO recommended coefficients (Etc(FAO)), and satellite image derived data (ETc\*).

However, in [4], it is also remarked that there are several alternative ways to obtain the coefficient  $K_c$  using different equations as it can be seen by looking at works such as [13], [14]. Briefly, in these studies it was shown that the different approaches had some advantages and drawbacks in terms of fitting the plants models under certain circumstances. A similar study on the crop coefficient  $K_c$  is done in [15], where the results are evaluated for different cases and species.

In our project, the use of NDVI to obtain a more accurate value of  $K_c$  is interesting as current literature in hazelnut orchards about the computation of this coefficient is lacking. Also, this methodology provides, as it can be seen in Figure 2, a crop coefficient that captures the actual phenological state of the plantation thanks to the data collected through the remote sensing technology and it is not forced to rely on more rigid standard coefficients such as FAO coefficients.

We expect that once a good approximation of the  $K_c$  coefficient will be obtained based on the data collected within the *Azienda Agricola Vignola*. Possibly, this formulation will be validated in other orchards of the Viterbo area.

#### 2.2.4 Irrigation

The **irrigation** inflow  $I$  highly depends on the irrigation system used and on the soil characteristics. For the selected experimental field used within PANTHEON, an underground drip irrigation system is available. Drip irrigation represents one of the most commonly used approaches for hazelnut farming. Compared to a sprinkler irrigation system, for drip irrigation systems the water is more concentrated in a unique point than spread out around a certain area. Therefore, to describe irrigation through drip irrigation system our finite-element discretization approach seems very appropriate.

In particular we assume that each parcel (node)  $i$  is obtained as the sum of all the contribution of all the watering points  $k$  available at that parcel  $i$ , that is:

$$I_i = \sum_{k \in J_i} I_{i,k} \quad (6)$$

where  $I_{i,k}$  denotes the watering point  $k$  available at the parcel  $i$  and  $J_i$  denotes the set of watering points available at parcel  $i$ . The most typical case is that the  $i$ -th plot will have one irrigation point or no irrigation point at all. In our model we assume that no water loss is experienced between the irrigation point and the plots. This can be explained by considering that the water is delivered at 30 cm depth and thus we can assume that surface runoff or evaporation do not affect water distribution.

#### 2.2.5 Rainfall

The **rainfall**  $R$  is the amount of water measured for a certain period of time on the soil. This term clearly varies depending on the climatic zone where the field belongs to and the period of the year.

Notably, since we are considering a finite-element discretization of the soil, it is important to consider how different parcels of the orchard are affected differently by the rain, depending on the plant coverage of a specific parcel. Inspired by [16] where precipitation is calculated depending on the values of the canopy covering every plot, we will consider a specific precipitation index for each parcel of our finite-element discretization of the field. In this regard, as trees in the orchard are separated and clearly not all the ground is covered by the plant, depending on how the precipitation is measured, a coefficient  $\varphi_i$  can be applied to every parcel (node)  $i$  (based on the trees canopy coverage for that parcel  $i$ ) in order to compute the rainfall for that specific node  $i$ , that is:

$$R_i = \varphi_i * R_{tot} \quad (7)$$

where  $R_{tot}$  is the amount of water per square meter assuming that there is no tree coverage. Future work will be focused on collecting data from the “Azienda Agricola Vignola” in order to identify the coefficient  $\varphi_i$  for the field selected within the PANTHEON project for the experimental validation.

#### 2.2.6 Surface runoff

**Surface runoff**  $SR$  is the quantity of water runoff from the surface of the soil. In several hydraulic models this term is neglected, as in [2], [3], according to the following assumptions: i) the field is completely flat and ii) no saturation condition on the soil occurs. For our setting, we are going to neglect this term as well based on the following considerations: i) an underground irrigation system is used and ii) the case of heavy rain is not very relevant for the goal of our model. This can be explained by the fact that under these two considerations

it is realistic to assume that there will not be an excessive amount of water applied to the soil, thus ensuring that no saturation will occur on the soil moisture level.

### 2.2.7 Deep percolation

**Deep percolation**  $P$  is the hydrological process where the water from the root zone moves downwards to a deeper level, where the plant cannot have access to it. According to [2], deep percolation is proportional to the soil moisture content of the soil  $\theta$  and the characteristics of the given soil denoted by the constant parameter  $C_s$  obtained from direct measurements. Therefore, within our setting where a finite-element discretization of the soil is considered, we can define the deep percolation  $P_i$  of a parcel  $i$  according to the following equation:

$$P_i = C_s * \theta_i \quad (8)$$

where  $\theta_i$  denotes the soil water storage for the parcel  $i$ . Future work will be focused on collecting data from the “Azienda Agricola Vignola” in order to identify the characteristic parameter  $C_s$  for the field selected within the PANTHEON project for the experimental validation.

### 2.2.8 Underground runoff

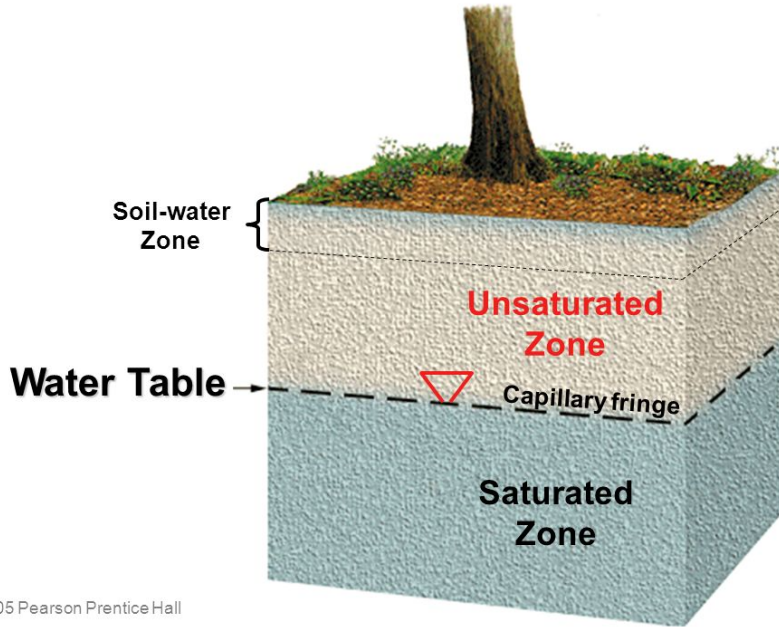
**Underground runoff**  $UG$  represents the horizontal movement of the underground water between different areas of the soil. In particular, within our setting where a finite-element discretization of the soil is considered, we can assume a redistribution of the underground water based on difference of water potential between neighbouring parcels. A similar approach can be seen in [17] [18]. Therefore, the underground runoff  $UG_i$  of the parcel  $i$  can be obtained according to the following equation:

$$UG_i = \eta * \sum_{k \in N_i} (\theta_k - \theta_i) \quad (9)$$

where  $\eta$  is a constant term related to water diffusivity in the soil, and  $N_i$  represents the set of neighbour parcels adjacent to the parcel  $i$ . Note that, to derive eq. (9) we have assumed that different parcels share the same soil characteristic, thus leading to a linear relation between the soil moisture content and the water flux between nodes. Future work will be focused on collecting data from the “Azienda Agricola Vignola” in order to identify the characteristic parameter  $\eta$  for the field selected within the PANTHEON project for the experimental validation.

### 2.2.9 Capillary rise

The **capillary rise**  $C$  occurs when the ground water stored in the soil saturated zone, called water table, is sucked upward by the soil root zone through small pores called capillaries. In these cases where those two



© 2005 Pearson Prentice Hall

Figure 3: Water table division.

layers are widely separated, capillary rise can be neglected, as in [2], [3]. In works like [4], [10] capillary rise is assumed to be negligible when the water table is more than 1 m below the bottom of the root zone. In this preliminary work, we assume the saturated zone to be deep enough to consider this term negligible also for the experimental field selected within the PANTHEON project. Future work will be focused on collecting soil moisture data from the “Azienda Agricola Vignola” in order to validate this assumption.

### 2.2.10 Soil moisture dynamics

In conclusion as a model for the soil dynamics we propose the following first-order continuous time modelling for each parcel  $i$  of the finite-time approximation of the soil:

$$\dot{\theta}_i = -ET_i + I_i + R_i - P_i + UG_i \quad (10)$$

which, considering the nature of the various phenomena described in the previous subsections can be written as

$$\dot{\theta}_i = -K_c * ET_o + I_i + \varphi_i * R_{tot} - C_s * \theta_i + \eta * \sum_{k \in N_i} (\theta_k - \theta_i) \quad (11)$$

We reiterate that this dynamical model, which describes the soil water storage dynamics for each parcel  $i$ , is the result of a sequence of simplifying assumptions. Future work will focus on the experimental validation of this model within the context of hazelnut orchards.

### 2.3 Water plant storage model

In this section, we model the dynamics of the water absorbed by a single plant.

We reiterate that our goal is to derive a general model to design a control law by considering both the water status of soil, the water status of each plant, and the way these two phenomena are coupled.

For the plant balance, we follow the same approach used to derive the soil water storage model. We denote with  $W$  with water stored by a plant. Accordingly, we consider the plant water storage variation  $\Delta S$  as the result of the plant water inflows  $S_{in}$  (water absorbed by the plant) minus the plant water outflows  $S_{out}$  (water lost by the plant), that is:

$$\Delta S = S_{in} - S_{out} \tag{12}$$

To quantify these water flows, we take inspiration from the electrical analogy presented in [5] (see Figure 4) where water potential and plant characteristics are used to compute the variation of the water flows in the plant. More specifically, by denoting with  $\dot{W}$  the variation of water stored by a plant, and by following the electrical analogy given in [5], the following differential equation can be derived:

$$\dot{W} = F_{tree} - E \tag{13}$$

where the water absorbed from the soil by the roots, denoted by  $F_{tree}$ , is considered as the inflow and the transpiration coming from the leaves, denoted by  $E$ , is considered as the outflow. Further parameters involved in this balance will be studied and added in case of significance.

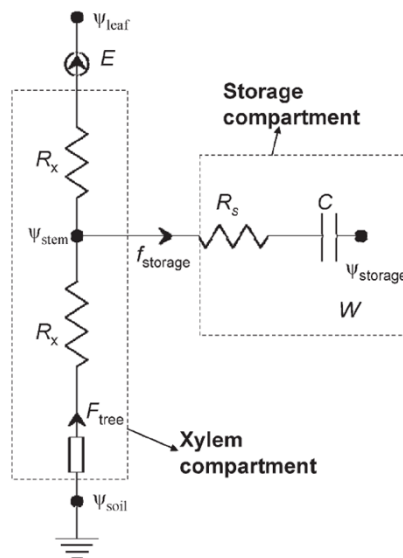


Figure 4: Electric equivalent of the plant model.

Inspired by [6], [19], [20] and by following the electrical equivalence shown in the Figure 4, in order to compute water absorbed by the plant ( $F_{tree}$ ) the following equation can be considered:

$$F_{tree} = \frac{(\Psi_{soil} - \Psi_{stem})}{R_x} \tag{14}$$

where the water absorbed by the plant, equivalently to Ohm's law, is a function depending on the water potential of the soil  $\Psi_{soil}$ , on the water potentials of the plant  $\Psi_{stem}$ , and on the resistance  $R_x$  exerted by stem and roots.

From the identification viewpoint, we expect to obtain the soil water potential  $\Psi_{soil}$  from the soil moisture balance applied to the different areas of the orchard and its combination with in situ measurements. This can be done by assuming a linear relation between soil moisture content  $\theta$  and water potential of the soil  $\Psi_{soil}$ , which leads to the following expression for the soil water potential  $\Psi_{soil}$ :

$$\Psi_{soil} = m_1 \theta(t) \tag{15}$$

Note that, in eq. (15) for the sake of generality we omit the dependence of the soil moisture content  $\theta$  from the parcel index as several different scenarios may occur. For example, a plant may draw water only from one parcel, then it would be  $\theta = \theta_i$ , or alternatively a plant may draw water from several parcels, then it would be  $\theta = \sum_{k \in H} \alpha_k \theta_k$  where  $H$  is the set of parcel indices associated with the tree.

As far as the water stem potential  $\Psi_{stem}$  is concerned, in [19] the authors obtained accurate results of plant water flow by simplifying the stem potential as a linear function of the water stored (see Figure 5) resulting in the following equation:

$$\Psi_{stem} = m_2 W(t) \tag{16}$$

At this point, by substituting in eq. (14) the expressions we derived for the soil water potential  $\Psi_{soil}$  and for the water stem potential  $\Psi_{stem}$ , we can rewrite the expression of the water absorbed by the plant  $F_{tree}$  as the combination of two functions depending on the soil water storage  $\theta$  and the plant water storage  $W$ , that is:

$$F_{tree} = c_2 \theta(t) - k_1 W(t) \tag{17}$$

where the stem resistance term  $R_x$  has been included in the constant parameters  $c_2$  and  $k_1$ , which can vary depending on the tree as it is shown in [19]. These constants should be estimated from field measurements depending on the soil composition and tree characteristics respectively [21].

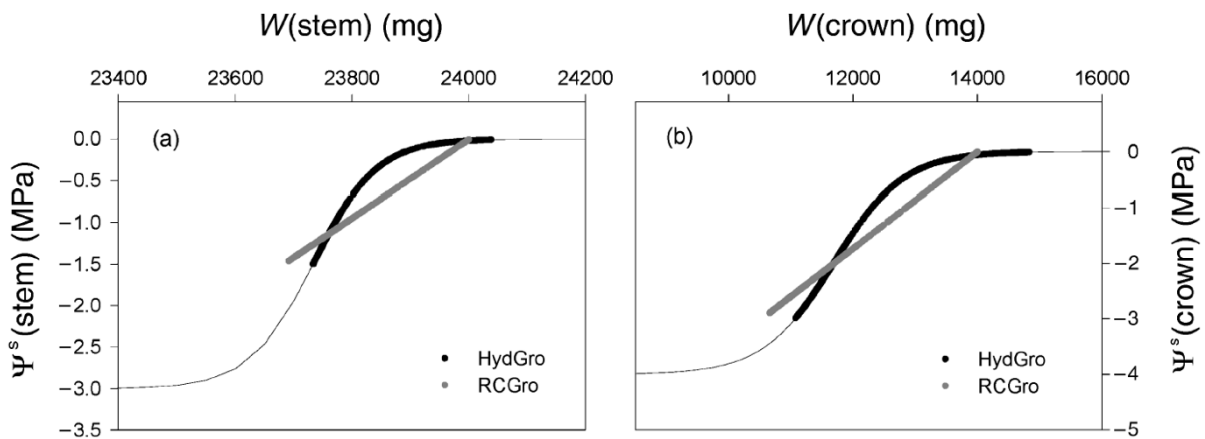


Figure 5: Linear approximation between water content and water potential for the stem and the crown

A similar operation can be done to obtain the water transpired from the leaves of the tree  $E$ , where  $R_x$  is considered to be the same for both stem and branches. As a result, the following equation is obtained to describe the water  $E$  transpired from the leaves of the tree:

$$E = \frac{(\Psi_{stem} - \Psi_{leaf})}{R_x} \quad (18)$$

17

where according to [19], [22] the leaf potential  $\Psi_{leaf}$  depends on the amount of water  $W$  stored by the plant and on the climate conditions represented by  $Et_o$ , resulting in the following equation:

$$\Psi_{leaf} = m_3W - c_5Et_o(t) \quad (19)$$

As a result, by plugging eqs. (16) and (19): within eq. (18) we obtain the following relationship:

$$E = k_2W(t) - c_5Et_o(t) \quad (20)$$

indicating that the transpiration  $E$  is a function of the water plant status  $W$  and the evapotranspiration  $Et_o$ , where it should be noticed that the constant parameter  $k_2$  groups constant terms  $m_2$  and  $m_3$ .

At this point, by combining together equations (17) and (20) within eq. (13) we obtain the following expression:

$$\dot{W} = c_2\theta(t) - c_3W(t) + c_6Et_o(t) \quad (21)$$

indicating that the variation  $\dot{W}$  of the plant water storage depends on the soil moisture status  $\theta$ , the current plant water status  $W$  and the evapotranspiration  $Et_o$ , while constant  $k_1$  and  $k_2$  are combined in  $c_2$ . Future work will be focused on an experimental validation of the effectiveness of this dynamical model for the plant water storage dynamics.

## 2.4 Overall Model

To describe the overall model of the orchard for the irrigation control problem, it is enough to combine the soil water storage model and the plant water storage model previously described. If we focus on the single plant the combined model can be seen as a two-tanks water flow modelling as depicted in Figure 7. In particular, based on this analogy the first tank, which represents the soil water storage, is filled by irrigation and rain, meanwhile evaporation and transpiration remove water from it; the second tank, which represent the plant water storage model, is filled by the absorption coming from the roots, while plant transpiration removes water from it.

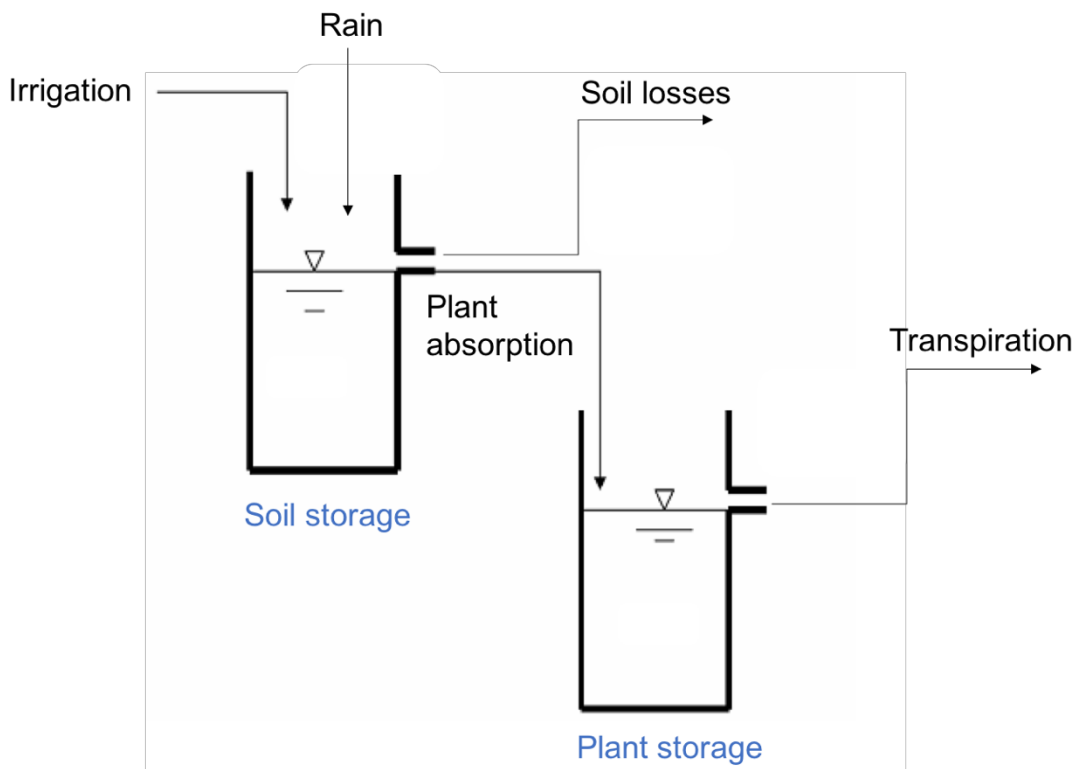


Figure 7: Tank model analogy

From a control theoretic perspective, this system (as show in Figure 8) can be represented as the combination of two processes where the irrigation is the control input, rain and evapotranspiration represent the disturbances affecting the system; and the output of the system is the quantity of water stored by the plant (analogue to the level of water in the second tank).

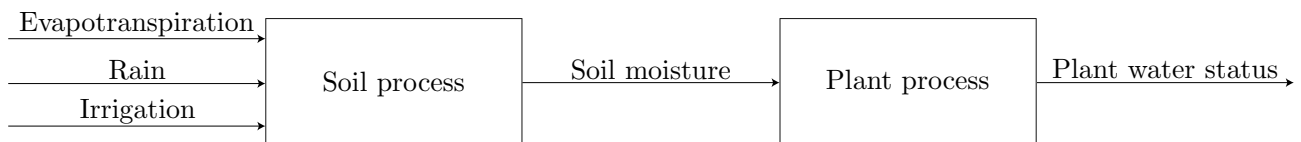


Figure 8: System description

It should be noticed that the disturbances in this process have a strong effect on the water balance dynamics of the system, and even if they cannot be controlled directly, we can obtain a fairly accurate model of the

main disturbances, namely rain and evapotranspiration, and apply control actions to our system as it is done in [2], [3] to comply with these disturbances.

Using this philosophy, we can model the entire orchard as follows.

As said, for the soil we have a collection  $V$  of  $N$  nodes that form a graph  $G = \{V, E\}$  where if the arc  $(v_i, v_j) \in E$  it means that the  $i$ -th node and the  $j$ -th node are neighbours. For the sake of notational simplicity, we will also define as  $N_i$  the set of neighbours of the  $i$ -th node.

Accordingly, we obtain the following dynamical model to describe the variation of the soil water storage for the parcel  $i$ :

$$\dot{\theta}_i = -c_1 * \theta_i + \sum_{k \in N_i} \eta_{k,i} (\theta_k - \theta_i) - c_{5,i} * ET_o(t) + \varphi_i * R_i(t) + I_i, i = 1, \dots, N \quad (22)$$

where the state variable  $\theta_i(t)$  denotes the soil moisture content in the soil parcel under analysis, the irrigation  $I_i$  is the irrigation input. Note that in eq. (22) the deep percolation is considered as a linear function of the soil moisture content  $\theta_i$ , and  $ET_o$  only depends on climate aspects.

Notably, this modelling based on the soil moisture balance has already been exploited in other works like [2], [3] where control actions were applied using a similar linear model obtaining satisfactory results. The main assumption here is that the soil is constantly within the limits of saturation and permanent wilting point, which gives a fairly linear behaviour of the soil dynamics. Compared to [2], [3], where a single variable of soil moisture is tracked for the whole orchard, the major novelty of this work as it will become clearer later is that for the derivation of the soil irrigation control process we are going to consider a finite-element approximation of the soil where the soil moisture balance will be computed for each parcel of the soil and coupling factors between neighbouring parcels will be considered.

As in previous works at the state of the art, e.g., [2], [3], the following assumptions are made to render the problem tractable:

- Soil moisture levels are always considered in the range between saturation and the permanent wilting point.

Water retention curve is considered linear. Which implies a linear relation between water quantity and water percolation by the soil.

For what regards the plants, we will denote as  $P$  the set of  $n$  plants that compose the orchard, and we will denote with  $V_j \subseteq V$  the set of nodes of  $V$  that contribute to provide water to the  $j$ -th plant. According to the previous analysis the dynamic of the  $j$ -th plant can be described as:

$$\dot{W}_j = \sum_{i \in V_i} c_{2,i,j} \theta_i(t) - c_{3,j} W_j(t) + c_{6,j} ET_o(t), j = 1, \dots, n \quad (23)$$

where the state variable  $W_j(t)$  represents the current water storage of the  $i$ -th plant. From (23), it can be noticed that the variation  $\dot{W}_j$  of the plant water storage depends on the soil moisture content, on the plant water storage  $W_j$  and on the evapotranspiration  $ET_o$ , which again is assumed to be only depending on climate aspects.

### 2.4.1 Overall Model: Including actuation

In the above described model nothing was said about sensing and actuators.

For what concerns actuators, with the currently used technology it is not very realistic to think that we have the capability to control each single water point  $I_i$ . What is much more realistic (and that actually reflects what is present in our test field) is that a single valve  $u_i$  commands an entire irrigation line/area insisting on several nodes. A possible way to model this is to define the set  $U_i$  of control inputs that insist on the same parcel node  $i$ , and to modify the equations as:

$$\dot{\theta}_i = -c_1 * \theta_i + \sum_{k \in N_i} \eta_{k,i}(\theta_k - \theta_i) - c_{5,i} * ET_o(t) + \varphi_i * R_i(t) + \sum_{k \in U_i} \xi_{i,k} u_k, i = 1, \dots, N \quad (24)$$

Where  $\xi_{i,k}$  is a gain quantifying the effect of the  $k$ -th input on the  $i$ -th parcel.

### 2.4.2 Overall Model: Including sensing

The two main kind of measurements of the water status that we will use in this project are:

- soil moisture sensors
- remote sensing based on the state of the leaves.

For what regard soil moisture sensors (with the needed adjustments) it is possible to measure directly the value of the soil moisture in a node  $\theta_i(t)$ . Thus, the  $j$ -th measured output  $y_j(t)$  representing a moisture sensor placed in a parcel  $i$ , it will assume the form  $y_j(t) = \theta_i(t)$ .

For what concerns the remote sensing, which is usually performed through UAVs, it is reasonable to assume that it allows (with some correction) to measure directly the plant water content at the level of the leaves. However, it is important to remark that there is typically a delay between the actual water content in the plant and the effect that it has in the water content in the leaves. As such we can assume that in reality if at a time  $t$  we have the leaf measurements concerning the  $j$ -th plant, what are we measuring is:

$$y_{remote,j}(t) = W_j(t - t_{delay}) \quad (25)$$

where as a first approximation in this deliverable we consider  $t_{delay} = 5$  hours for the numerical simulations. By resorting to fundamental results of control system theory, we know the delay can be seen in terms of transfer function as:

$$Y_j(s) = e^{-st_{delay}} W_j(s) \quad (26)$$

Furthermore, since this delay function is a transcendent function and represents itself an approximation, for the sake of simplicity and with no lack of generality, it is convenient to consider an approximation of this function by means of rational functions. In particular, by resorting to the Padé approximants we obtain:

$$e^{-st_{delay}} \approx \frac{-\frac{t_{delay}}{2}s + 1}{\frac{t_{delay}}{2}s + 1} \quad (27)$$

Note that, this can be equivalently expressed in state space as:

$$\dot{y}_{remote,j}(t) = -\frac{2}{t_{delay}} y_{remote,j} + \frac{2}{t_{delay}} W_j(t) - \dot{W}_j(t) \quad (28)$$

At this point it should be noticed that, unlike moisture sensors, remote sensing is not always available, but data is available only when a flight is performed. Future work will be focused extending the mathematical modelling in order to consider this observation.

### 2.4.3 Overall Model - Equations

Putting together the equation for the overall orchard, and assuming we have  $N$  parcels and  $n$  plants, we obtain the following linear dynamical model:

$$\begin{aligned} \dot{\theta}_i &= -c_{1,i} * \theta_i + \sum_{k \in N_i} \eta_{k,i} (\theta_k - \theta_i) - c_{5,i} * ET_o(t) + \varphi_i * R_i(t) + \sum_{k \in U_i} \xi_{i,k} u_k, i = 1, \dots, N \\ \dot{W}_j &= \sum_{i \in V_i} c_{2,i,j} \theta_i(t) - c_{3,j} W_j(t) + c_{6,j} Et_o(t), j = 1, \dots, n \\ \dot{y}_{remote,j}(t) &= -\frac{2}{t_{delay}} y_{remote,j} + \left( \frac{2}{t_{delay}} + c_{3,j} \right) W_i(t) - \sum_{i \in V_i} c_{2,i,j} \theta_i(t) - c_{6,j} Et_o(t), j = 1, \dots, n \end{aligned} \quad (29)$$

It is important to remark that this model has a very large number of parameters that will have to be identified. However, on the basis of the previous description of the model, we expect that it is possible to determine all of them by using a relatively low number of measurements coupled with the knowledge of the geometry of the orchard. In particular:

- for what concerns the terms  $\eta_{k,i}$  we expect that they will be the same for all parcels when the field is homogeneous (as in our case study). For other cases, as soon as data will be available, we will try to formulate easy rules (e.g. based on relative altitude and relative composition of the soil);
- for what concerns  $c_{5,i}$  and  $\varphi_i$ , in this phase we believe it is enough to compute their value for a few “uncovered plot” and then for each plot multiplying the “uncovered” value with a factor between 0 and 1 proportional to the percentage of covering of the plot due to the tree crown;
- $\xi_{i,k}$  will have the same numerical value for all parcels, whereas  $U_i$  only depends on the knowledge of the irrigation system, which is known a priori;
- For what concerns  $c_{2,i,j}$  it is reasonable to define it as a linear function of the quantities of roots of the plant  $i$  in the plot  $j$ . This quantity can be well approximated by the fact that, in a hazelnut, the crown distribution is a good approximation of the roots distribution;
- $c_{3,j}$  and  $c_{6,j}$  are the same for all plants (under the assumption of  $W_i$  normalized w.r.t. the plant size).

#### 2.4.4 Overall Model: The single soil parcel - single plant model

To make some tests and gain insights on how the control for this kind of system should be performed, we also introduce a single soil parcel - single plant model, which becomes a two-state model in the form:

$$\begin{bmatrix} \dot{\theta}(t) \\ \dot{W}(t) \end{bmatrix} = \begin{bmatrix} -c_1 & 0 \\ c_2 & -c_3 \end{bmatrix} * \begin{bmatrix} \theta(t) \\ W(t) \end{bmatrix} + \begin{bmatrix} c_4 \\ 0 \end{bmatrix} * I(t) + \begin{bmatrix} -c_5 \\ -c_6 \end{bmatrix} * Et_o(t) + \begin{bmatrix} \varphi \\ 0 \end{bmatrix} * R(t) \quad (30)$$

where  $\theta$  and  $W$  are the two state variables,  $I$  is the input of our system and  $R$  and  $Et_o$  are system disturbances.

We reiterate that in deriving this second-order model, we have assumed: i) the system to be operating always within the saturation limits, ii) the equations to be linear and iii) the values depending on the stomatal resistance of the plant or the soil composition to be constant during the whole process.

For what regard the sensing we will assume (depending on the needs) that is possible to have both soil moisture sensors (and thus to directly measure  $\theta$ ), and remote sensing based on the leaves (from now on denoted as leaf measurements), which eventually leads to the following dynamical system with three state variables:

$$\begin{bmatrix} \dot{\theta}(t) \\ \dot{W}(t) \\ \dot{y}_{remote}(t) \end{bmatrix} = \begin{bmatrix} -c_1 & 0 & 0 \\ c_2 & -c_3 & 0 \\ -c_2 & \frac{2}{t_{delay}} + c_3 & -\frac{2}{t_{delay}} \end{bmatrix} \begin{bmatrix} \theta(t) \\ W(t) \\ y_{remote}(t) \end{bmatrix} + \begin{bmatrix} c_4 \\ 0 \\ 0 \end{bmatrix} I(t) + \begin{bmatrix} -c_5 \\ -c_6 \\ c_6 \end{bmatrix} Et_o(t) + \begin{bmatrix} \varphi \\ 0 \\ 0 \end{bmatrix} R(t) \quad (31)$$

### 3 Control Techniques for Irrigation

In this section, based on the dynamical models derived in Section 2, control techniques for the irrigation problems will be presented. In particular, first the irrigation control problem for the single soil parcel – single plant water storage model is addressed, successively the irrigation problem for the finite-element representation of the entire orchard is discussed.

#### 3.1 Single Soil Parcel - Single Plant Water Storage Model

In this section different control strategies are proposed for the single soil parcel - single plant water storage dynamical model discussed in Section 2.4. The goal of this study is to gain insight on the structure that the irrigation control should have, so as to guide the future research on the irrigation of the entire orchard.

This section is organized as follows. First the model parameters along with a description of disturbances used for the simulations are discussed. Successively, a proportional control scheme under the assumption of leaf measurements availability is presented. Next, a proportional control scheme under the assumption of both leaf measurements and soil moisture measurements availability is described. Then, an observer-based state-feedback control based only on the assumption of leaf measurements availability is introduced. Finally, a comparison of the proposed control strategies is given, and their advantages and limitations are discussed.

##### 3.1.1 Model Parameter Selection and Evapotranspiration Data

In this section, we first describe the parameters selected for the proposed single soil parcel - single plant water storage dynamical model; then we described the evapotranspiration data collected in the area of Viterbo, Italy, that will be used as disturbances for the simulations.

As described in Section 2, the following third order dynamical system is used for the single soil parcel - single plant model:

$$\begin{bmatrix} \dot{x}_1(t) \\ \dot{x}_2(t) \\ \dot{x}_3(t) \end{bmatrix} = \begin{bmatrix} -c_1 & 0 & 0 \\ c_2 & -c_3 & 0 \\ -c_2 & \frac{2}{t_{delay}} + c_3 & -\frac{2}{t_{delay}} \end{bmatrix} \begin{bmatrix} x_1(t) \\ x_2(t) \\ x_3(t) \end{bmatrix} + \begin{bmatrix} c_4 \\ 0 \\ 0 \end{bmatrix} I(t) + \begin{bmatrix} -c_5 \\ -c_6 \\ c_6 \end{bmatrix} Et_o(t) + \begin{bmatrix} \varphi \\ 0 \\ 0 \end{bmatrix} R(t) \quad (32)$$

where  $x_1 = \theta$  represents the soil moisture,  $x_2 = W$  the water stored in the plant, and  $x_3 = y_{delay}$  is the state representing the water measured at the leaves level. It is assumed that  $t_{delay} = 5$  hours.

For the simulations, the following constant parameters were considered:

- $c_1$ : Depending on the deep percolation and other possible factors that make water runoff.
- $c_2$ : Grouping the terms for the soil potential considering that in the operating point it follows a linear distribution with constant  $c_2$ .
- $c_3$ : Grouping the terms for the plant and leaves water potential.
- $c_4$ : Depending on the position of the parcel respect to the irrigation line. Currently it is 1 for simplicity, considering that all water coming from irrigation is absorbed by the terrain.
- $c_5$ : Representing the crop factor of the orchard. It modifies the reference evapotranspiration obtained from Montheit-Penman equation.
- $c_6$ : Representing the effect of the evapotranspiration on the plant water content.
- $\varphi$ : Depending on the canopy cover for that area. It represents the amount of rain that reaches the soil area.

In particular, the constant terms associated to irrigation and rain are assumed as  $c_4=1$  and  $\varphi=1$ . Note that, this implies that all the water provided by the irrigation system and by the rain is absorbed by the soil. This assumption was made also in [3] to simplify the exposition.

The value of the coefficient  $c_5$ , as detailed in [10], depends on the period of the year and the typology of orchard. By exploiting the coefficients derived in [12] for hazelnut plantation, we obtain  $k_c=[0.2100; 0.2200; 0.2300; \mathbf{0.3}; \mathbf{0.4}; \mathbf{0.62}; \mathbf{0.7}; \mathbf{0.55}; \mathbf{0.35}; \mathbf{0.2500}; 0.2200; 0.2000]$ ; where the entry  $i$ -th entry of the vector denotes the value of the coefficient for the  $i$ -th month of the year. In our case, only the coefficients in bold are necessary (from March to October) as the rest of the year the trees are considered to be in rest and irrigation is not applied [23].

The parameter  $c_2$  was calculated using values from [5] and  $c_6$  is firstly considered as  $-0.01$  to study its effect on the system. When data from the experimental field are going to be available, these values will be replaced by measurements from the orchard.

The last parameter,  $c_1$ , depends on the soil composition and it is usually calculated through in situ measurements of the soil. This value is considered as  $c_1=0.003$  per hour which means around  $0.45$  mm/h of percolated water (considering soil moisture values within 150-300 mm). This term, compared to the different values cited in [24], a study of soil composition, describes a reasonable behaviour for a standard orchard.

Note that, for the dynamical model of the plant water storage, due to the lack of data availability, we have used parameters coming from [5] where the authors attempted to model the dynamics of peach trees. Similarly, for the dynamical model of the soil water storage, due to the lack of data availability, values coming from the literature were used. Future work will be focused on the identification of proper coefficient for the hazelnut crop.

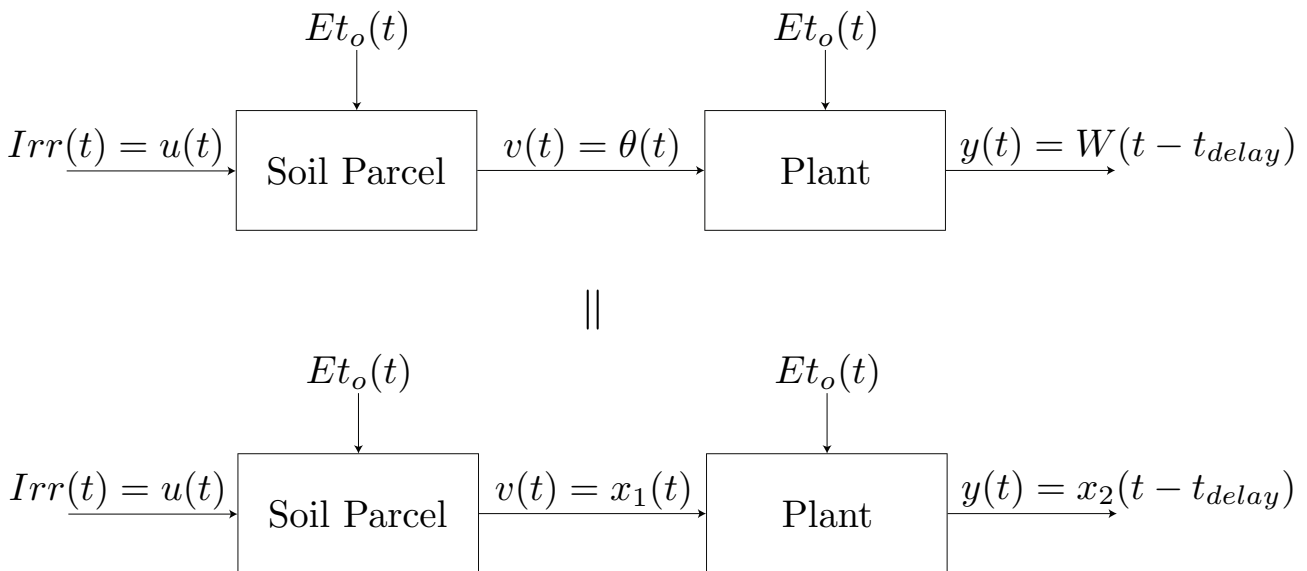


Figure 9 – Block Diagram of the Single Soil Parcel - Single Plant Dynamical Model

Figure 9 depicts the block diagram representation of the proposed single soil parcel – single plant dynamical model where it should be noticed the fact that the control term is the irrigation  $Irr(t) = u(t)$ , the state variables are respectively the soil water storage and the plant water storage, and the output is represented by the data  $y(t) = W(t - t_{delay})$  coming from leaf measurements and (possibly) from soil moisture measurements  $v(t) = \theta(t)$ . Furthermore, it can be noticed the presence of the evapotranspiration  $Et_o(t)$  encoding the system disturbances.

Figure 10 depicts the impulse response for the single soil parcel – single plant dynamical model computed by exploiting the selected parameters discussed so far. In particular, it can be noticed the stable nature of the system, meaning that under the assumption no input signal is given, that is no irrigation is given, the amount of water stored by the soil and the plant reasonably tends to zero.

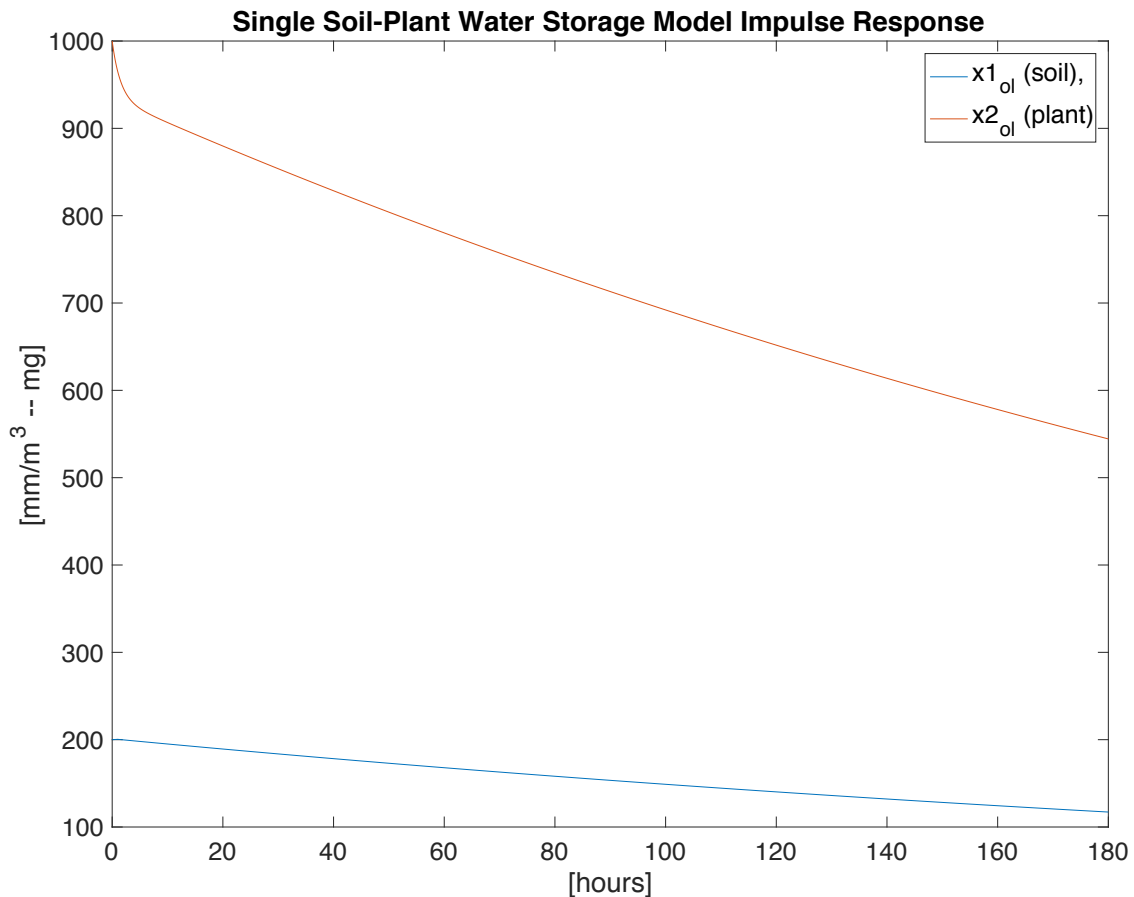


Figure 10 - Impulse Response

To evaluate the robustness of the proposed control strategies against environmental disturbances, data collected from a meteorological station located in Viterbo (near to the experimental area) is considered. We resorted to the Monteith-Penman equation introduced in [10] to obtain reference values for the evapotranspiration. This would allow to simulate disturbances which are compatible with the climatic conditions of the selected experimental field within the “Azienda Agricola Vignola”. For the sake of simplicity, only evapotranspiration is considered as a disturbance for running the simulations. In Figure 11 we can observe the evapotranspiration  $Et_o(t)$  registered in the area of Viterbo during two weeks of April 2018 that will be used for the simulations.

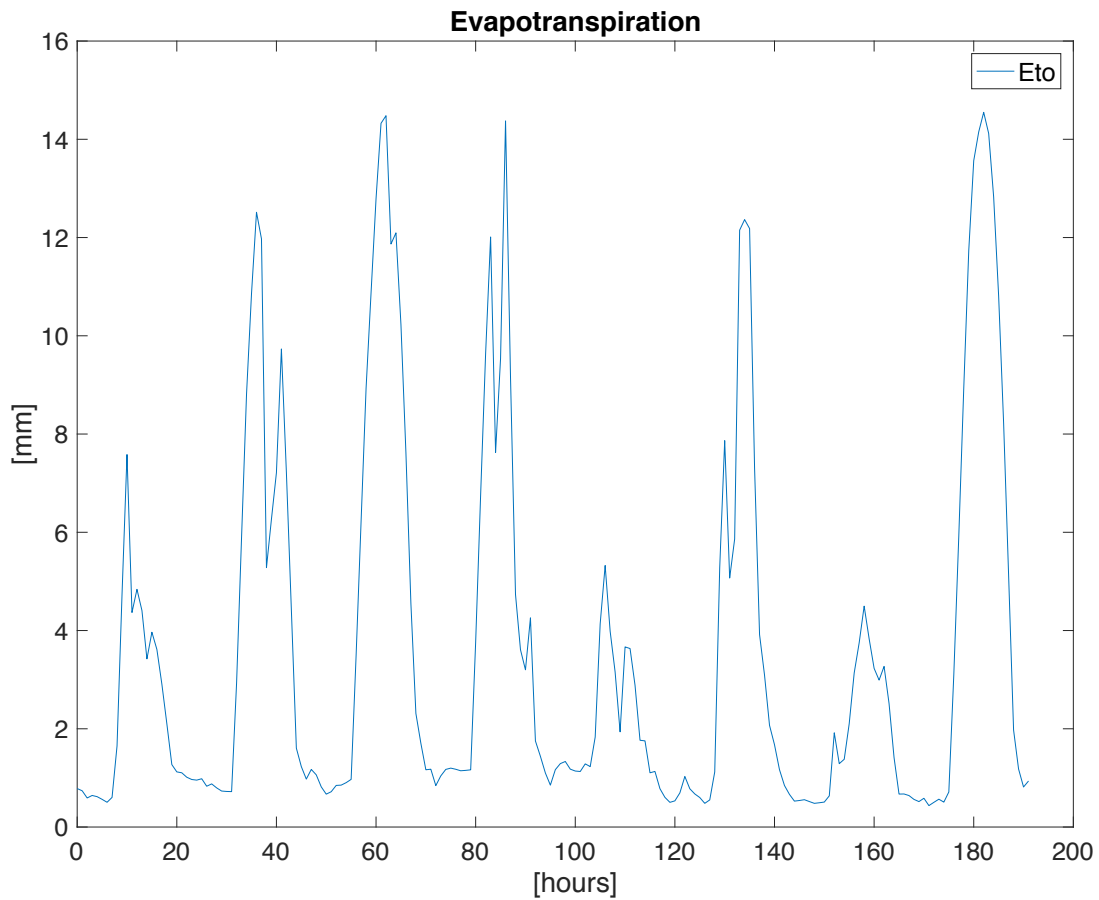


Figure 11 – Evapotranspiration Data collected from Viterbo Area

### 3.1.2 Proportional Controller based on Leaf Measurements

In this section, we proposed a simple proportional control scheme under the assumption of leaf measurements availability. In particular, we numerically demonstrate how the delay in collecting information about the amount of water stored by the plant due to the leaf measurements negatively impact the robustness of the control strategy in the disturbances occur. Furthermore, we numerically demonstrate how even under the assumption of partial rejection of the disturbances, that is by assuming that noisy measurements of the evapotranspiration are available, the proposed control scheme still does not behave satisfactory.

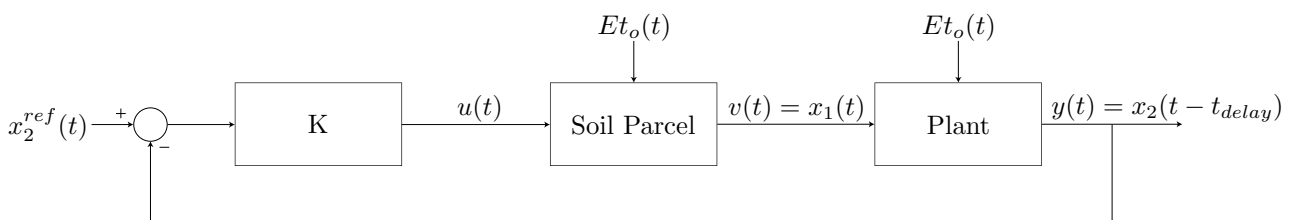


Figure 12 - Block Diagram of the Control Strategy based on Leaf Measurements

Figure 12 depicts the closed-loop system based on the proposed proportional control strategy. In particular, it should be noticed how the feedback loop compares the reference value  $x_2^{ref}(t)$  describing the desired

amount of water to be stored by the plant at time  $t$  with the measurement  $y(t) = x_3(t) = x_2(t - t_{delay})$  describing at time  $t$  the amount of water that was stored by the plant at time  $t - t_{delay}$ .

Figure 13 depicts the outcome of a simulation for the closed-loop dynamical system based on the proposed proportional control law under the assumption that no disturbances occur. In particular, the evolution of the two state variables  $x_1(t)$  and  $x_2(t)$  is presented along with the reference value  $x_2^{ref}(t)$ . It can be noticed how in this nominal case where no disturbances occur, the state variable  $x_2(t)$  can get sufficiently close to the reference value  $x_2^{ref}(t)$  over time, that is  $x_2(t) - x_2^{ref}(t) \approx 0$  as  $t \rightarrow \infty$ . Thus, implying that the performance of the control action is satisfactory, or in other words that the plant water storage has reached the desired level.

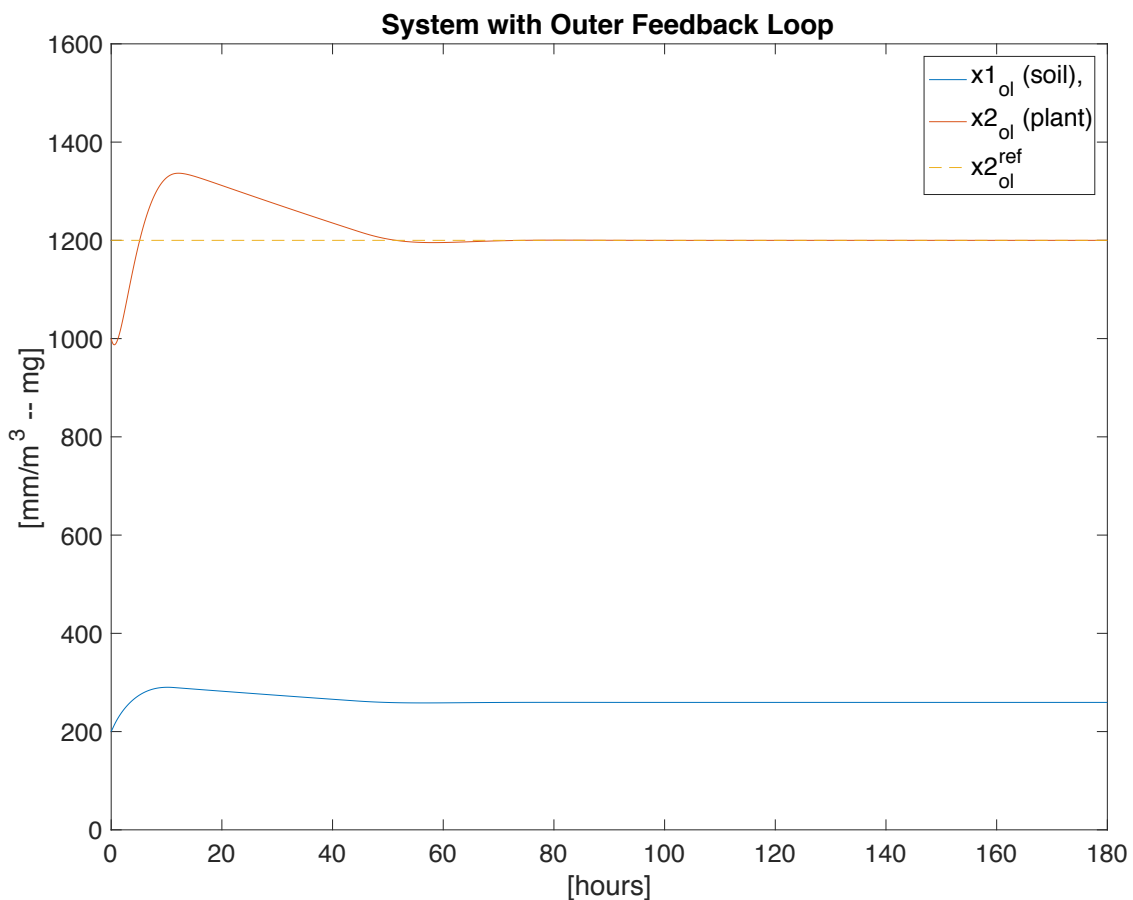


Figure 13 - Outer Loop with No Disturbances

Figure 14 depicts the outcome of a simulation for the closed-loop dynamical system based on the proposed proportional control law by considering the presence of the evapotranspiration phenomenon as disturbances. We point out that values for the evapotranspiration are obtained as detailed in Section 3.1.1 (see Figure 11 for a graphical representation of the evapotranspiration over time). In particular, it can be noticed how in this case, due to the delay in retrieving information about the amount of water stored by the plant, the control strategy does not perform very well. This can be intuitively explained by the fact that due

to the delay introduced by the leaf measurements, the control law attempts to regulate now the amount of water that the plant had before.

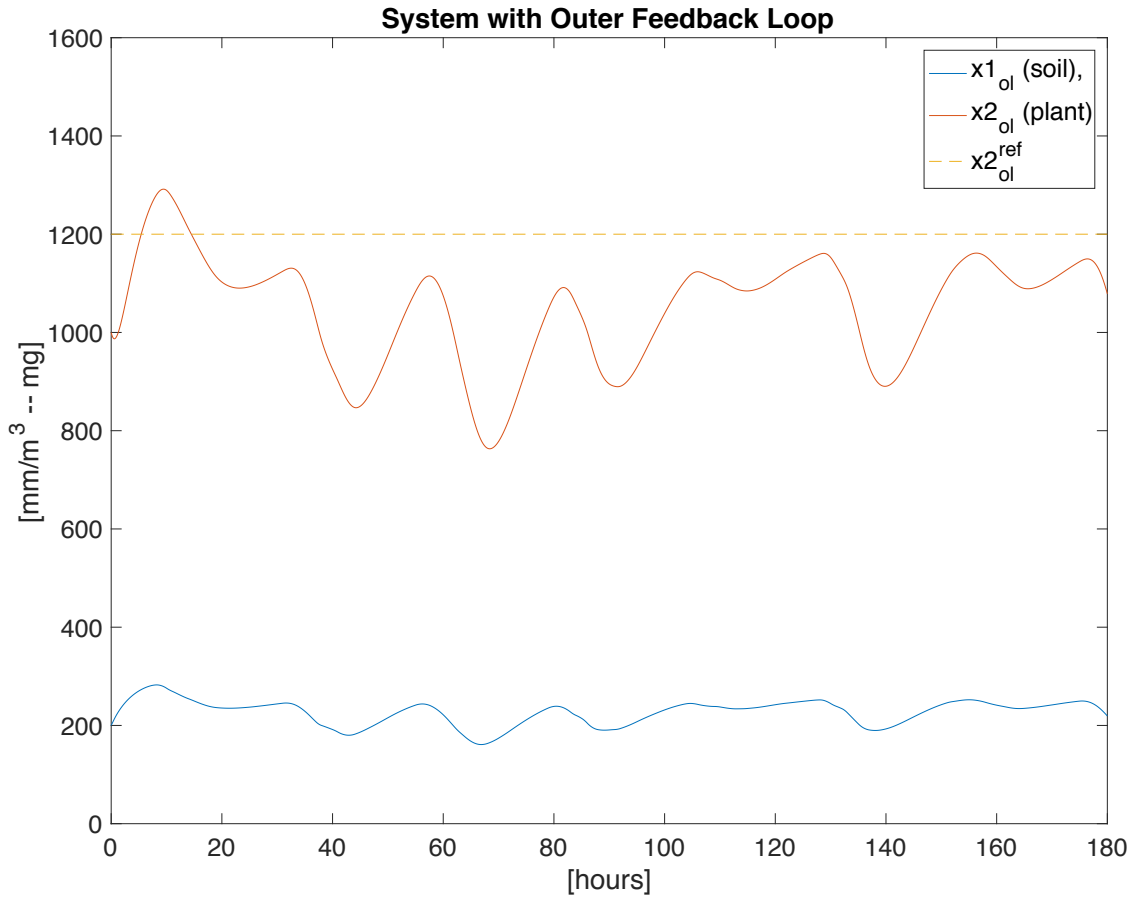


Figure 14 - Outer Loop with Disturbances

In order to mitigate this problem, a possible solution is to introduce a feed-forward control term which attempts to mitigate the effects of the evapotranspiration by rejecting the disturbance. Indeed, this is a reasonable assumption as the evapotranspiration can be measured by resorting to remote sensing technologies, e.g. through a weather station. However, we should point out that in a realistic setting it is realistic to assume noisy measurements and thus a perfect rejection cannot be achieved anyway. For this reason, in the simulation for the feed-forward term we have considered an additive noise to the evapotranspiration measurements up to 20% of the maximum amplitude of the evapotranspiration signal itself to prevent perfect rejection.

Figure 15 depicts the outcome of a simulation for the closed-loop dynamical system based on the proposed proportional control law with a feed-forward control term on the noisy measurements of the evapotranspiration. In particular, it can be noticed how even though the performances improve compared to the case without disturbances measurements, the performances of the control architecture are still quit not satisfactory, that is the value of the state variable  $x_2(t)$  not get sufficiently close to the reference value  $x_2^{ref}(t)$  over time, thus indicating that the amount of water stored by the plant does not reach the desired value.

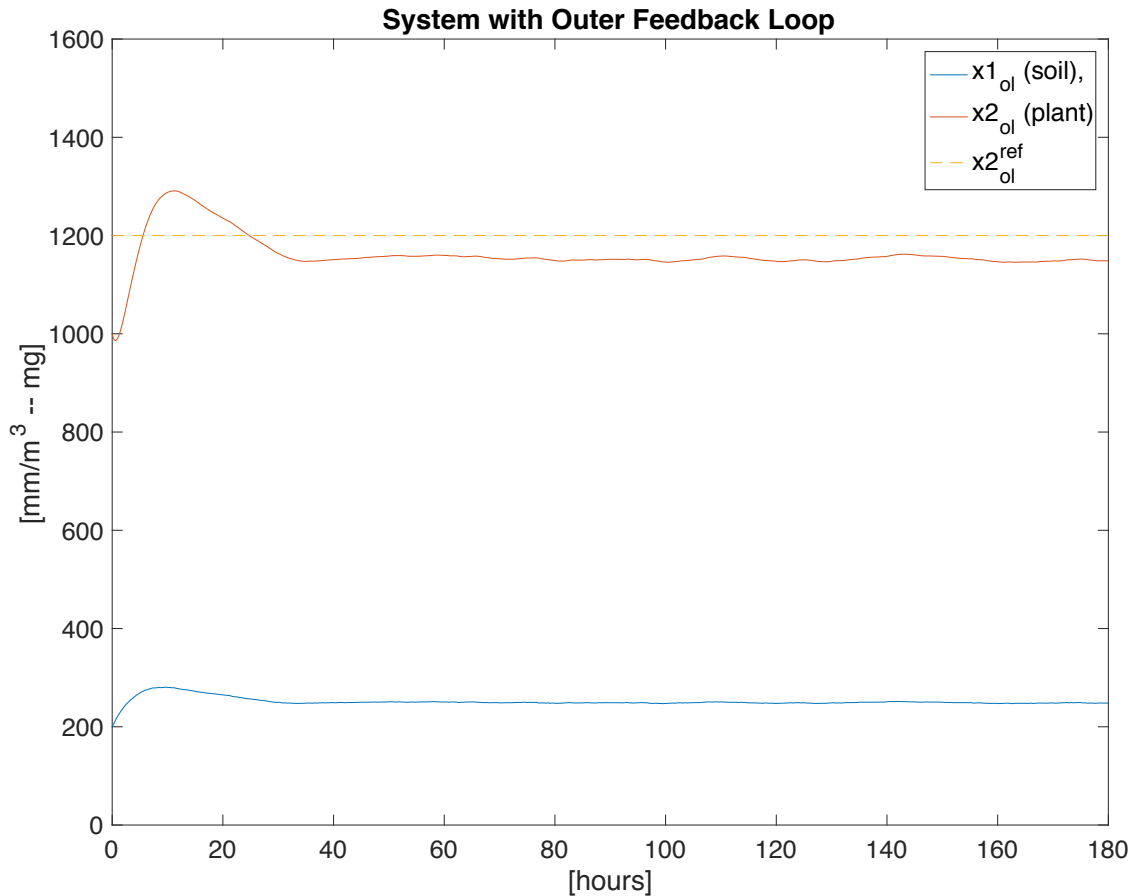


Figure 15 - Outer Loop with Partial Disturbances Rejection

### 3.1.3 Proportional Controller based on Leaf Measurements and Soil Moisture Measurements

In this section, motivated by the observations collected in Section 3.1.2 regarding the lack of robustness of the proposed control law against the presence of disturbances, we propose an alternative control strategy based on the assumption that both leaf measurements and soil moisture measurements are available. Indeed, as it will become clear later in this section, this control techniques proves more effective, especially in the case of partial disturbances rejection. Intuitively, the idea underlying this control strategy is that since the delay in the soil moisture measurements can be considered negligible, the resulting control law can be tuned more aggressively to reject disturbances; thus, proving particularly effective to mitigate the effects of noisy evapotranspiration measurements that prevents the feed-forward control term to achieve perfect disturbances rejection.

Figure 16 depicts the closed-loop system based on the proposed proportional control strategy. In particular, it can be noticed that two control loops are considered: i) an outer control loop that compares the reference

value  $x_2^{ref}(t)$  describing the desired amount of water to be stored by the plant at time  $t$  with the measurement  $y(t) = x_3(t) = x_2(t - t_{delay})$  describing at time  $t$  the amount of water stored by the plant at time  $t - t_{delay}$ ; and ii) an inner control loop that compares the control input  $u(t)$ , describing the current control action required to reach the desired amount of water to be stored by the plant at time  $t$  with the current value of the state variable  $x_1(t)$ , describing the current amount of water stored in the soil.

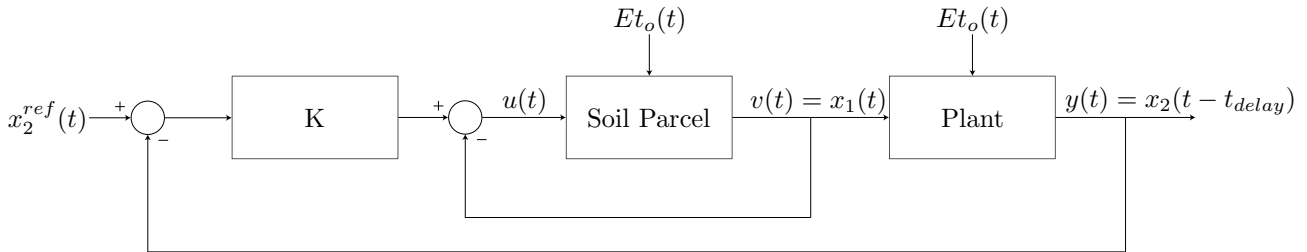


Figure 16 - Block Diagram of the Control Strategy based on Leaf Measurements and Soil Moisture Measurements

Figure 17 depicts the outcome of a simulation for the closed-loop dynamical system based on the proposed proportional control law under the assumption that no disturbances occur. In particular, the evolution of the two state variables  $x_1(t)$  and  $x_2(t)$  is presented along with the reference value  $x_2^{ref}(t)$ . As for the control law discussed in Section 3.1.2, it can be noticed how also for this control strategy, in the nominal case where no disturbances occur, the reference value  $x_2^{ref}(t)$  can be reached by the state variable  $x_2(t)$ ; thus, implying that the performance of the control action is satisfactory.

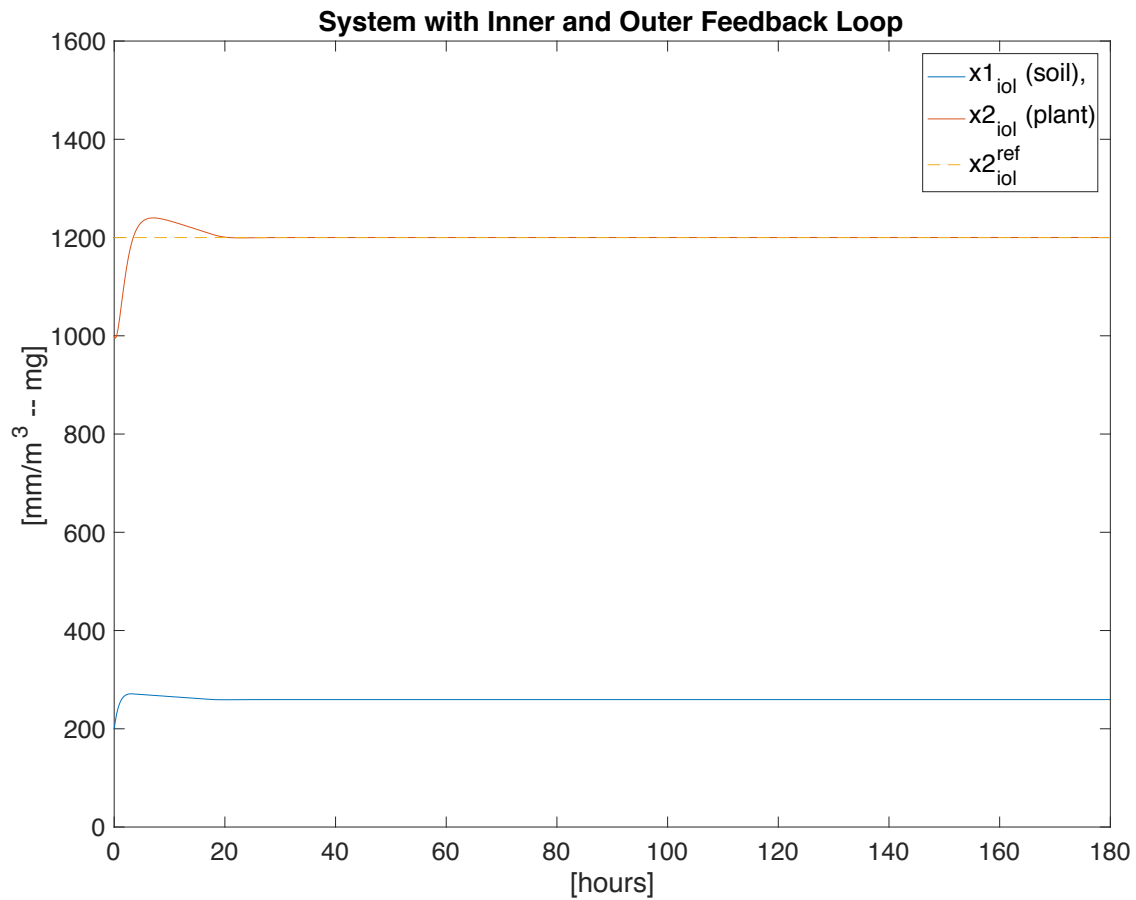


Figure 17 - Inner Outer Loop with No Disturbances

Figure 18 depicts the outcome of a simulation for the closed-loop dynamical system based on the proposed proportional control law by considering the evapotranspiration as disturbances. As for the simulations presented in Section 3.1.2, values for the evapotranspiration  $Et_o$  are obtained according to eq. (3) as described in Section 3.1.1 (see Figure 11 for a graphical representation of the evapotranspiration over time). In particular, it can be noticed how, thanks to the availability of the inner control loop, better performances can be achieved compared to the control law presented in Section 3.1.2. Nevertheless, results are not quite satisfactory yet. Thus, indicating also in this case the need of a feed-forward control term, which attempts to mitigate the effects of the evapotranspiration by rejecting the disturbance.

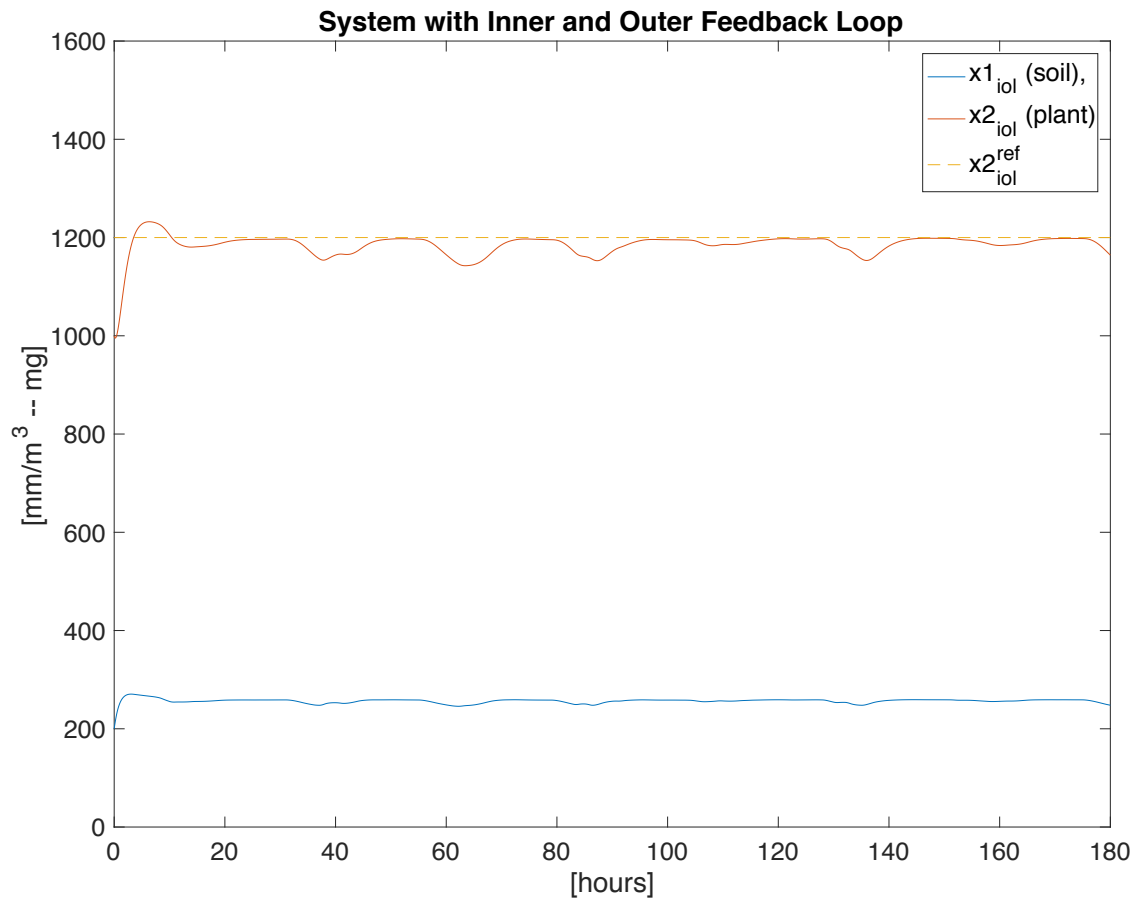


Figure 18 - Inner and Outer Loop with Disturbances

Figure 19 depicts the outcome of a simulation for the closed-loop dynamical system based on the proposed proportional control law with a feed-forward control term on the noisy measurements of the evapotranspiration. In particular, it can be noticed how, thanks to the availability of the inner control loop, better performances can be achieved, compared to the control law presented in Section 3.1.2 where only leaf measurements were available. Interestingly, it can be noticed how with the addition of the feed-forward control term this control scheme can provide similar performances to the nominal case without disturbances (and without feed-forward term). In other words, with this control strategy the state variable  $x_2(t)$  can get sufficiently close to the reference value  $x_2^{ref}(t)$  over time despite of the presence of noise affecting the evapotranspiration measurements. Thus, indicating that the proposed control scheme is a promising solution with good disturbance rejection capabilities.

However, it is worth to mention that from an implementation standpoint the major shortcoming of the proposed control strategy is the assumption of soil measurements availability. As a matter of fact, when looking at the problem at full scale, that is a setting involving a large-scale orchard with many hazelnut plants, this would imply that ideally a soil moisture sensor should be available for each parcel from which any tree draws water from. Clearly, this assumption implies a remote sensing infrastructure the cost of which does not seem sustainable. For this reason, in the next section we provide an alternative solution which allows to

maintain the good performances of the proposed strategy while alleviating the cost necessary for the implementation of the remote sensing infrastructure.

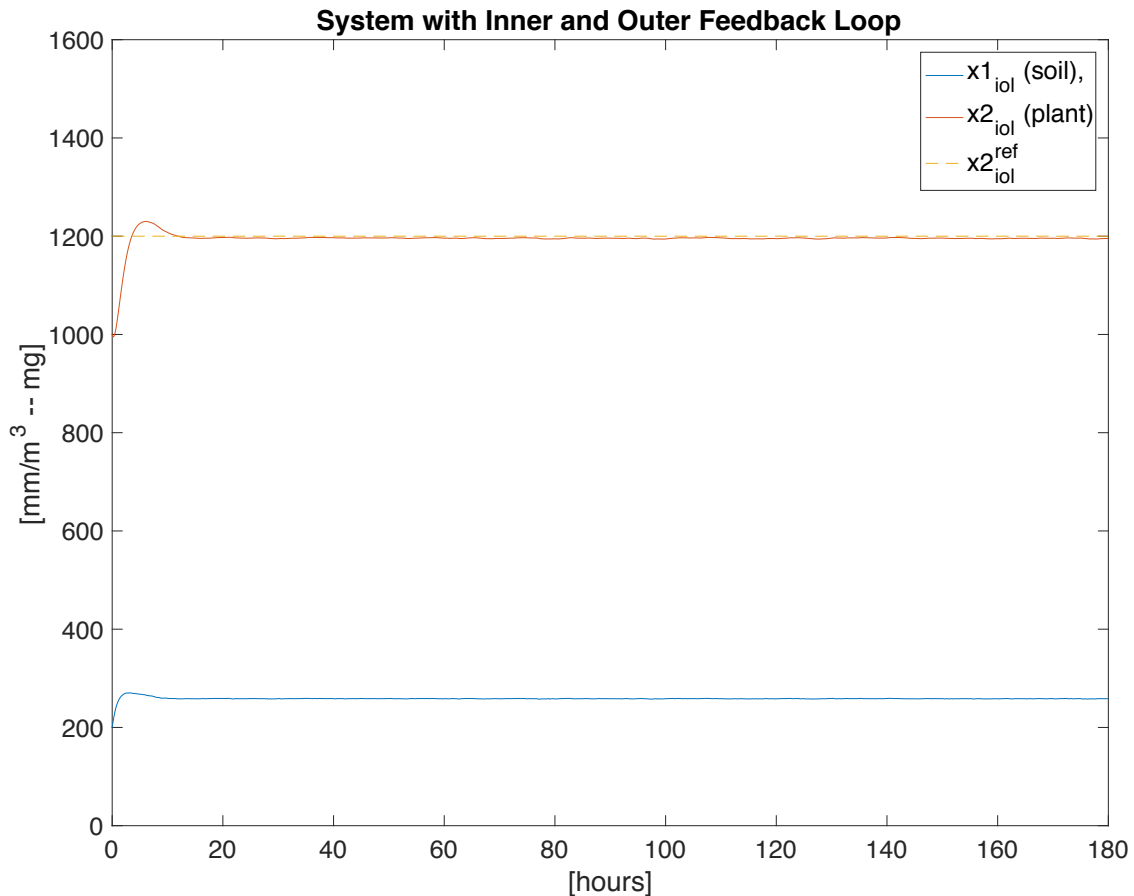


Figure 19 - Inner and Outer Loop with Partial Disturbances Rejection

### 3.1.4 Observer-based Control Design based on Leaf Measurements

In this section, motivated by the observations collected in Section 3.1.3 regarding: i) the good disturbances rejection performances of the control strategy by assuming both leaf and soil moisture measurements availability, and ii) the fact that as it is, the economic impact of this control strategy, in terms of infrastructure required for the implementation, would not be sustainable, we provide an alternative control strategy which can significantly cut the costs of the required infrastructure while still providing disturbances rejection performances which are comparable with the control strategy proposed in Section 3.1.3. Intuitively, the idea of this control strategy is that rather than exploiting a soil moisture sensor to measure the amount of water stored by the soil, we can introduce an additional control term, i.e., a state observer, which allows to estimate this information. Indeed, this can be achieved thanks to the structural observability property of the single soil parcel – single plant dynamical system under the assumption of sole leaf measurements availability.

Briefly, in control theory, a state observer is a system that provides an estimate of the internal state of a given real system, from measurements of the input and output of the real system. It is typically computer-implemented and provides the basis of many practical applications. The reader is referred to classical textbooks on linear state-space control theory such as [25] for further information on this topic.

Figure 20 depicts the closed-loop system based on the proposed observer-based state feedback control strategy. In particular, it can be noticed that two control loops are considered: i) an outer control loop which compares the reference value  $x_2^{ref}(t)$ , describing the desired amount of water to be stored by the plant at time  $t$  with the current value of the observer state variable  $\hat{x}_2(t)$ , describing an estimate of the amount of water  $x_2(t)$  stored by the plant at time  $t$ ; and ii) an inner control loop which compares the control input  $u(t)$ , describing the current control action required to reach the desired amount of water to be stored by the plant at time  $t$  with the current value of the observer state variable  $\hat{x}_1(t)$ , describing an estimate of the current amount of water  $x_1(t)$  stored in the soil.

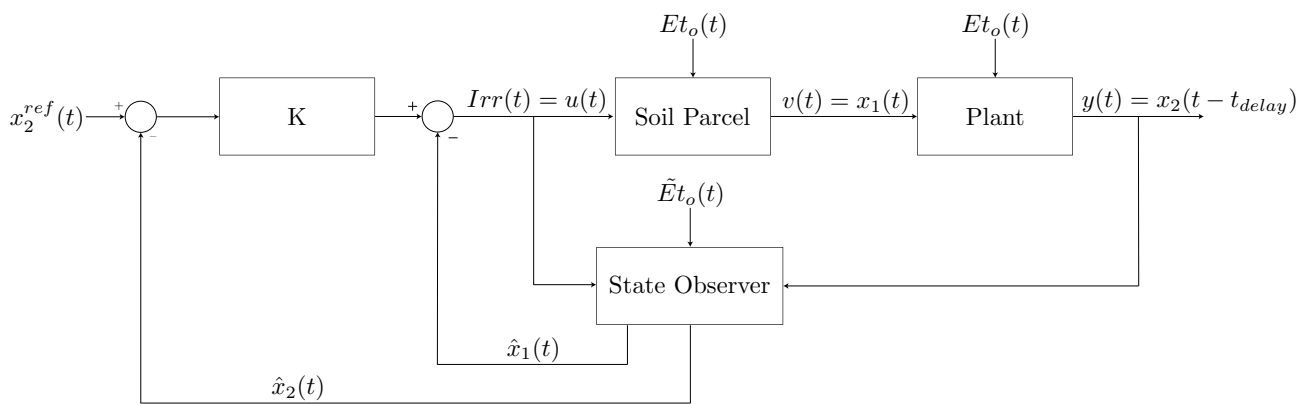


Figure 20 - Block Diagram of the Observer-based Control Design based on Leaf Measurements

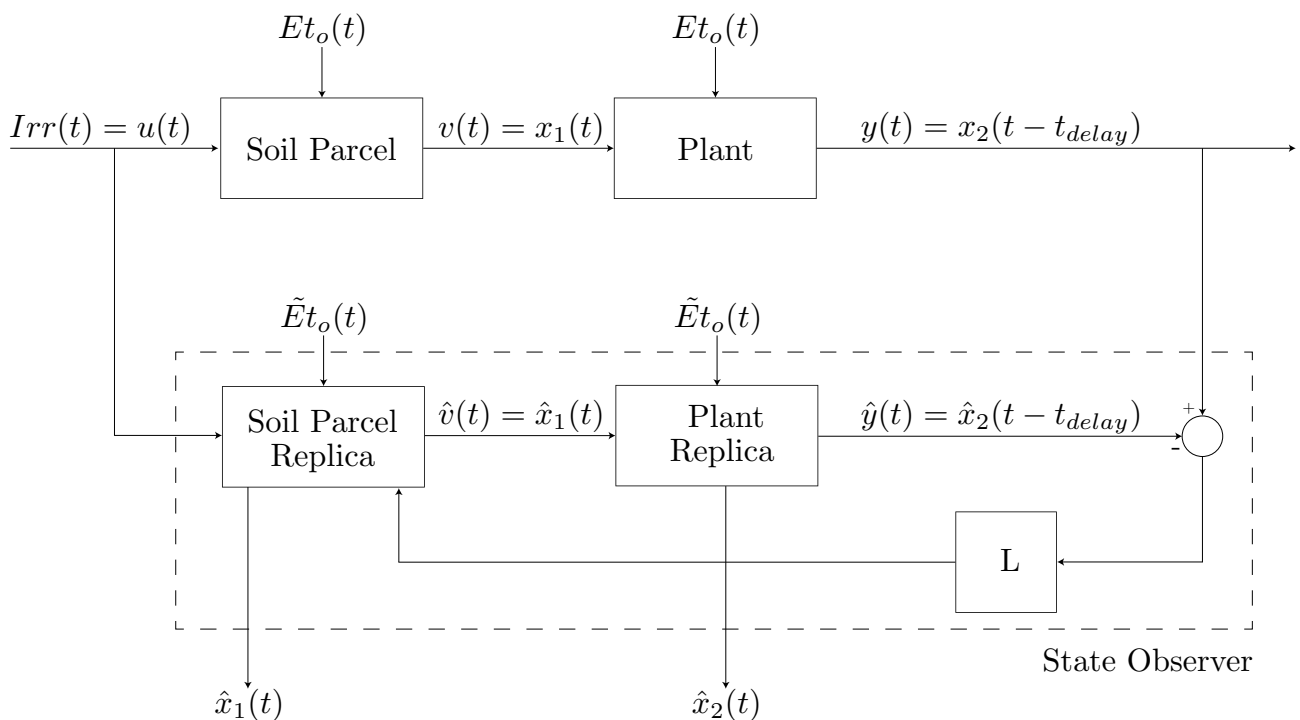


Figure 21 - Block Diagram of the Structure of the State Observer Dynamical System

Figure 21 depicts the structure of the state observer. In particular, it can be noticed how the dynamical system describing the state observer “embeds a copy” of the mathematical modelling of the real system, that is in our case the single soil parcel – single plant dynamics. In addition, it should be noticed the presence of an additional dynamical system to model the delay in obtaining information concerning the amount of water stored by the plant due to the leaf measurements.

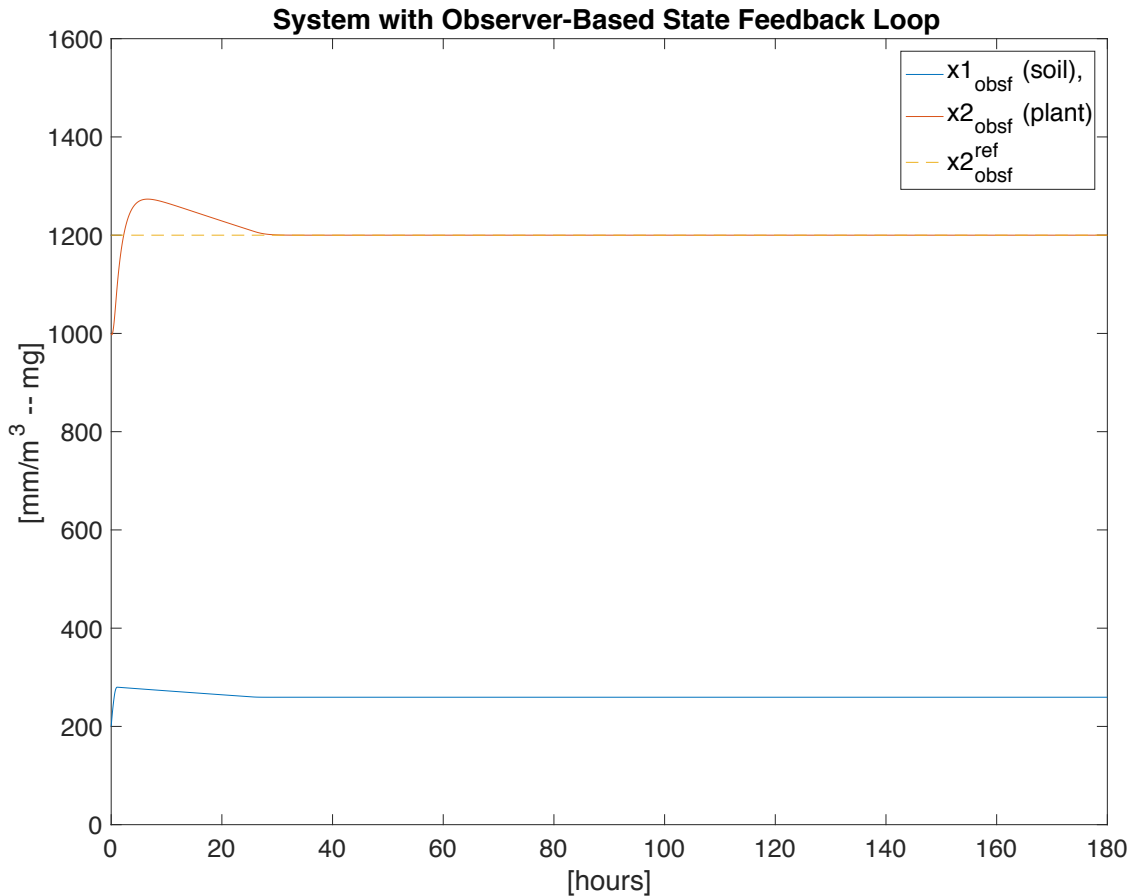


Figure 22 - Observer-based State Feedback with No Disturbances

Figure 22 depicts the outcome of a simulation for the closed-loop dynamical system based on the proposed observer-based state feedback control law under the assumption that no disturbances occur. In particular, the evolution of the two state variables  $x_1(t)$  and  $x_2(t)$  is presented along with the reference value  $x_2^{ref}(t)$ . As for the control laws discussed in Section 3.1.2 and Section 3.1.3, it can be noticed how also for this control strategy, in the nominal case where no disturbances occur, the reference value  $x_2^{ref}(t)$  can be reached by the state variable  $x_2(t)$ ; thus, implying that the performance of the control action is satisfactory.

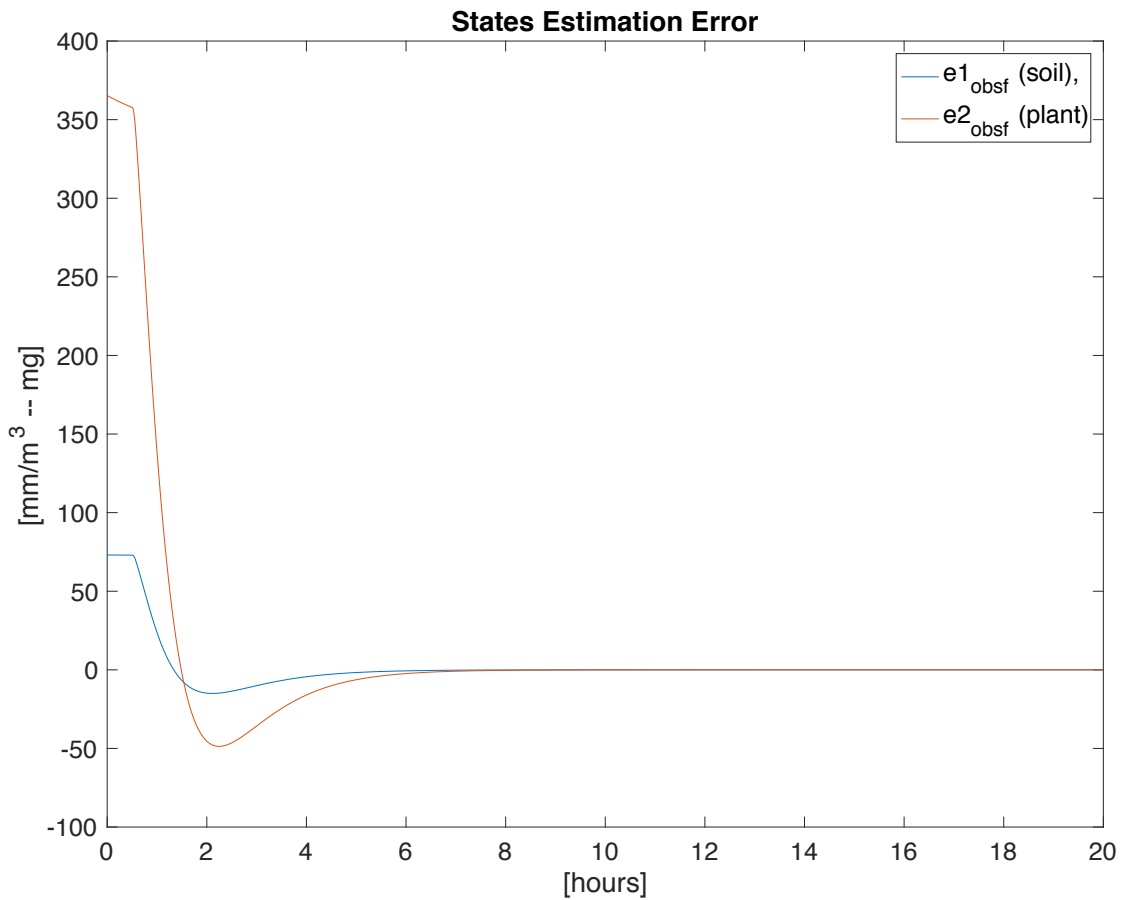


Figure 23 - State Estimation Error with No Disturbances

Figure 23 depicts the state estimation error for this simulation involving the proposed observer-based state feedback control law under the assumption that no disturbances occur. In particular, it can be noticed how for the proposed state observer the state-estimation error becomes negligible very quickly, thus indicating that after a short amount of time the state-feedback control term closed by the state estimates behaves as if the control law had direct access to the state variables of the physical system. Interestingly, this control strategy offers also the advantage that the outer loop is no longer closed by a delayed information coming from the leaf measurements, i.e.,  $y(t) = x_2(t - t_{\text{delay}})$ , but rather by an accurate estimate of the physical state variable at time  $t$ , i.e.,  $\hat{x}_2(t) \approx x_2(t)$ .

Figure 24 depicts the outcome of a simulation for the closed-loop dynamical system based on the proposed observer-based state feedback control law by considering the evapotranspiration as disturbances. As for the simulations presented in Section 3.1.2 and in Section 3.1.3, values for the evapotranspiration are obtained as detailed in Section 3.1.1 (see Figure 11 for a graphical representation of the evapotranspiration over time). In particular, it can be noticed how the performances of this control strategy are very similar to the one obtained in Section 3.1.3 under the assumption of both leaf measurements and soil moisture measurements availability.

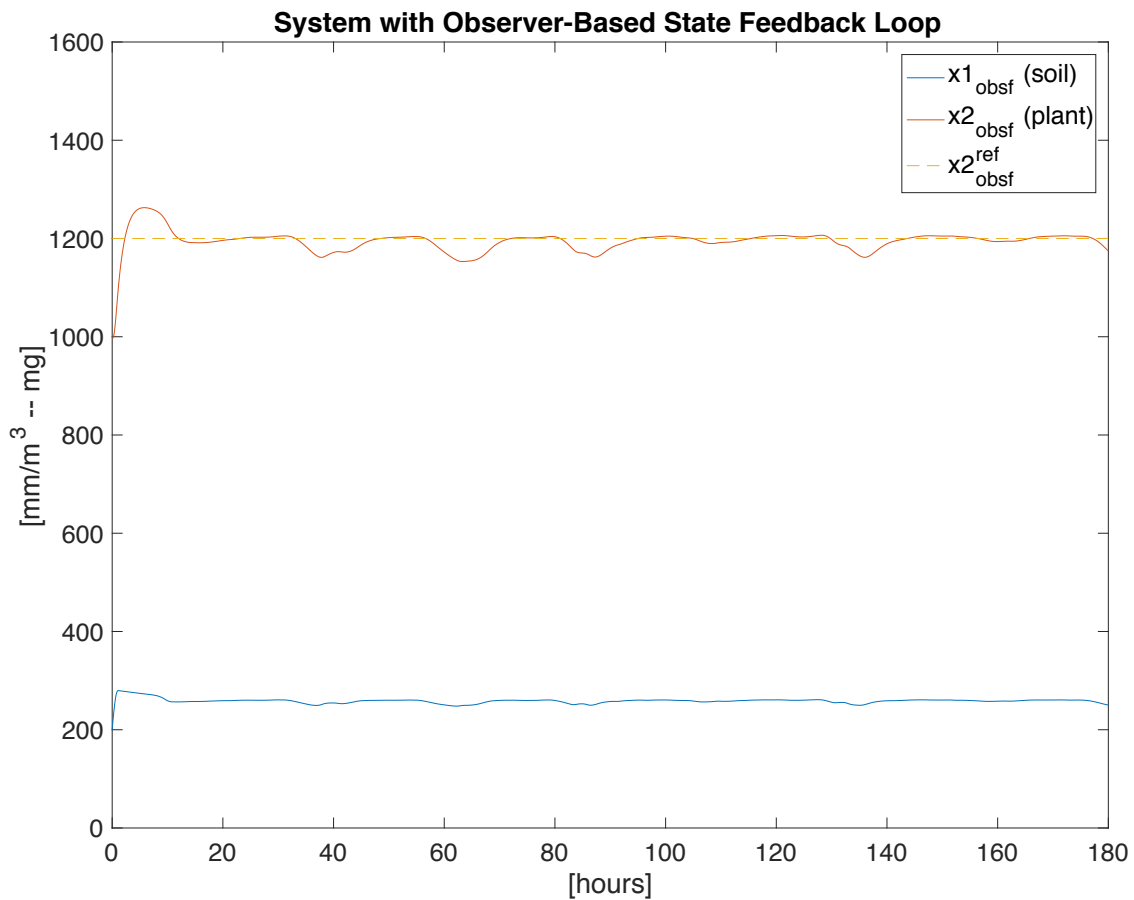


Figure 24 - Observer-Based State Feedback with Disturbances

Indeed, this can be explained by looking at Figure 25, which depicts the state estimation error for this simulation involving the proposed observer-based state feedback control law by considering the evapotranspiration as disturbances. In particular, according to the figure the estimation error becomes negligible very quickly, thus indicating that after a short amount of time the state-feedback control term closed by the state estimates behaves as if the control law had direct access to the state variables of the physical system. Nevertheless, as already mentioned in Section 3.1.3 results are not quite satisfactory yet. Thus, indicating also in this case the need of a feed-forward control term, which attempts to mitigate the effects of the evapotranspiration by rejecting the disturbance. Note that from an implementation standpoint,

simulations for this setting have been carried out under the assumption of noisy evapotranspiration measurements availability, which is necessary for a correct implementation of the state observer.

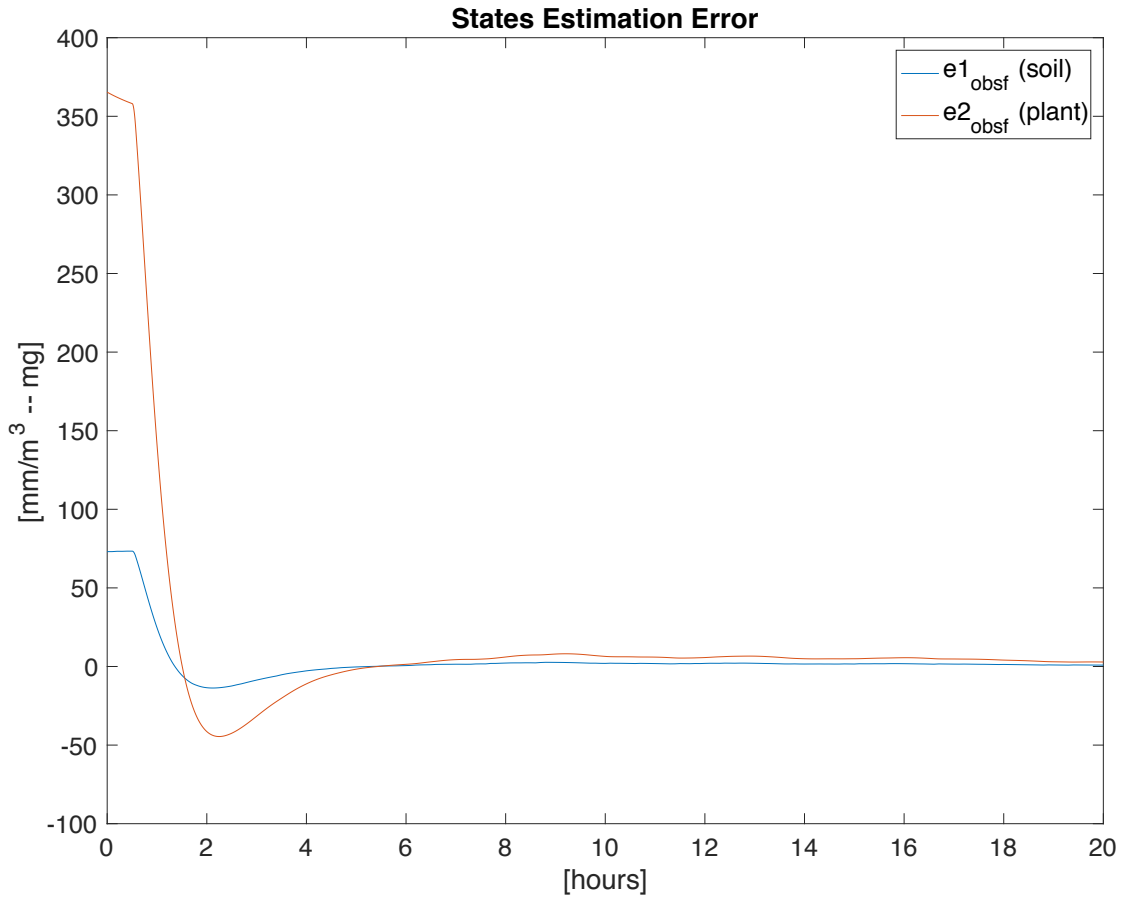


Figure 25 - State Estimation Error with Disturbances

Figure 26 depicts the outcome of a simulation for the closed-loop dynamical system based on the proposed observer-based state feedback control law with a feed-forward control term on the noisy evapotranspiration measurements. In particular, it can be noticed how the performances of this control strategy are quite similar to the one obtained in Section 3.1.3, which operates under the assumption of both leaf measurements and soil moisture measurements availability with a feed-forward term as well on the noisy evapotranspiration measurements.

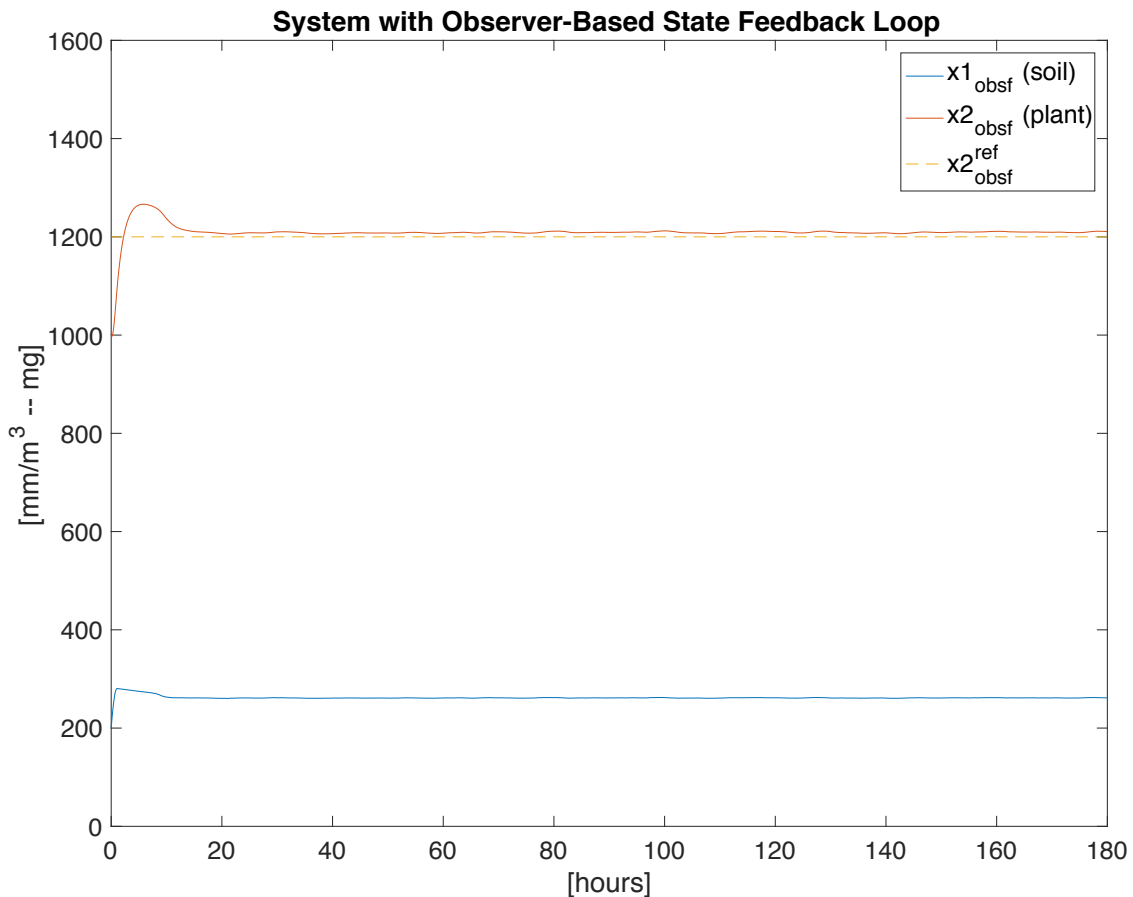


Figure 26 - Observer-Based State Feedback with Partial Disturbances Rejection

Indeed, as for the previous simulation, also in this case this can be explained by looking at Figure 27, which depicts the state estimation error for this simulation involving the proposed observer-based state feedback control law by considering the evapotranspiration as disturbances. More specifically, as for the previous simulation, the estimation error becomes negligible very quickly, thus indicating that after a short amount of time the state-feedback control term closed by the state estimates behaves as if the control law had direct access to the state variables of the physical system. Furthermore, as for the control strategy discussed in Section 3.1.3, it can be noticed how with the addition of the feed-forward control term this control scheme can provide similar performances to the nominal case without disturbances (and without feed-forward term), that is the state variable  $x_2(t)$  can get sufficiently close to the reference value  $x_2^{ref}(t)$  over time despite of the noise affecting the evapotranspiration measurements. Indeed, this indicates that the proposed control scheme represents a promising alternative to the control strategy discussed in Section 3.1.3, as it permits

to significantly cut the costs of the infrastructure deployment while still providing comparable disturbances rejection performances.

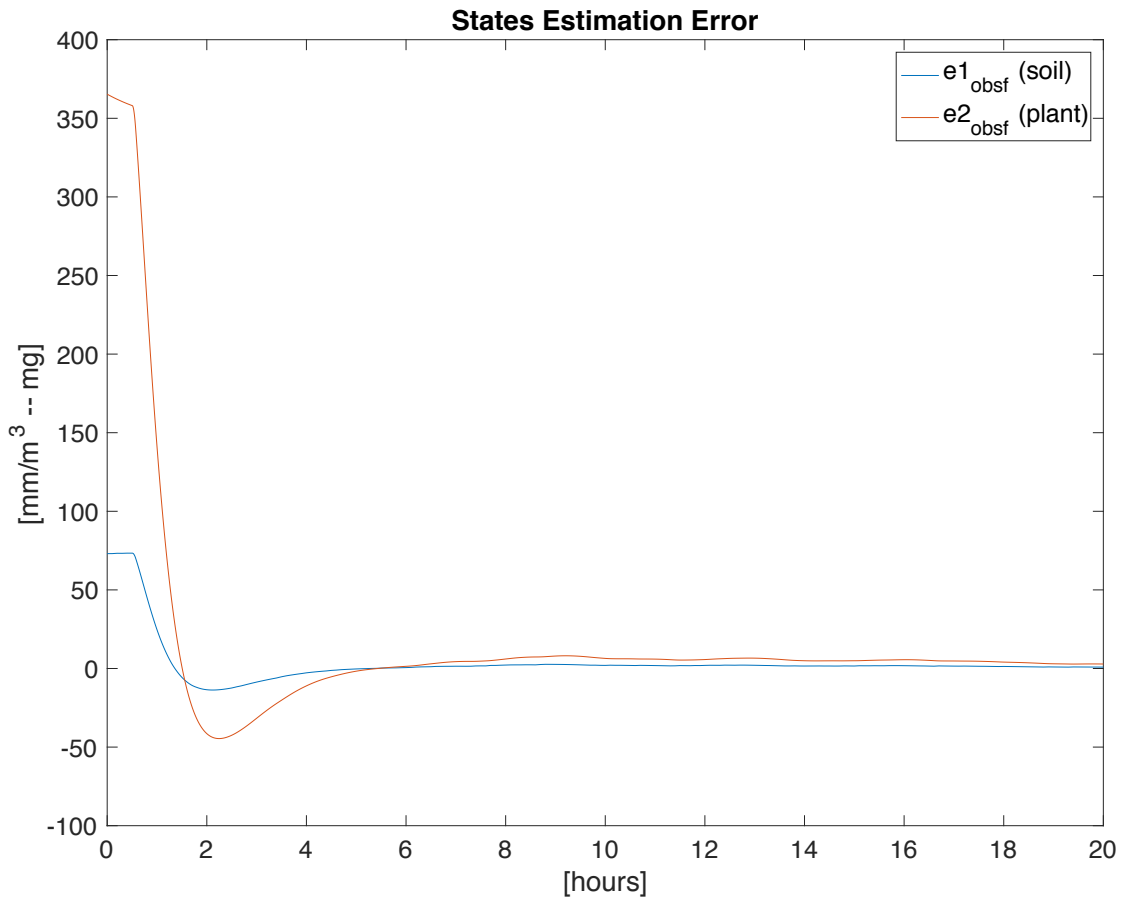
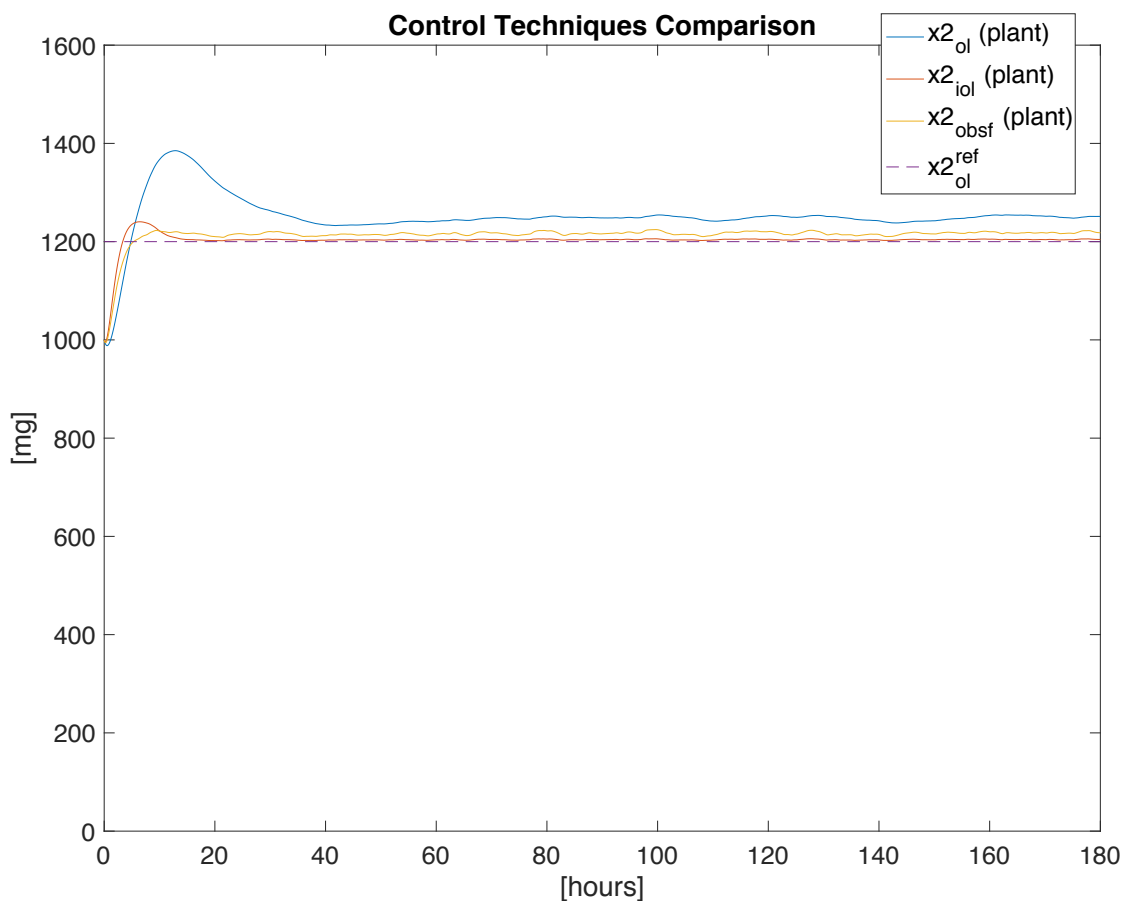


Figure 27 - State Estimation with Partial Disturbances Rejection

### 3.1.5 Performances Comparison

In this section, we provide a comparative evaluation of the performances of the proposed three control methodologies in order to emphasize their advantages and limitations. In particular, for the sake of readability and with no lack of generality, we focus only on the simulation setting involving the availability of noisy measurement of the evapotranspiration. Figure 28 depicts the outcome of a simulation for the closed-loop dynamical system for the three proposed control strategies by considering the availability of noisy measurements of the evapotranspiration. Note that, as explained in the previous sections, for each of the proposed control strategies a feed-forward control term is introduced to mitigate the effects of the evapotranspiration by partially rejecting the disturbance. In particular, it can be noticed how the first control strategy, based on a proportional control term under the assumption of only leaf measurements, provides reasonable worst performances compared to the other control strategies.



**Figure 28** - Control Techniques Comparison with Partial Disturbances Rejection

As far as the second and the third control strategies are concerned, no significant difference in the system behaviour can be noticed after their settling time. In addition, it can also be noticed that the second strategy exhibits a larger maximum overshoot value compared to the third one. Although for different simulations this can change as it strongly depends on the quality of the initial conditions for the state observer, that is it depends on how close these state variable values are from the actual state variable values of the physical system, in general under the assumption that good initial conditions for the state observer are available, that is sufficiently close to the actual values of the state of the physical system, this can be explained by the fact that the third control law does not suffer from the delayed information induced by the leaf measurements

as the outer control loop is based on the value of the estimate of the state water plant storage rather than on the delayed measurements provided by the leaves.

### 3.2 Controlling the Entire Orchard

#### 3.2.1 Insights from the Control of the Single Soil Parcel - Single Plant Water Storage and Preliminary Discussion

The preliminary analysis carried out in Section 3.1, although very simplistic, provides a series of insights that are very important to guide the definition of a control strategy for the entire orchard. In particular it shows that:

- a simple feedback based only the remote sensing is fragile with respect to environmental changes;
- the presence of soil moisture probes can greatly improve the control (and in particular the robustness);
- the feed-forward actions are important to give a first counteraction of the environmental changes;
- in absence of soil moisture probes, a state observer plus a static feedback can greatly improve the performance;

In summary, this preliminary activity on the Single Soil Parcel - Single Plant Water Storage strongly advocates for a system theoretic approach to the control of irrigation.

In other words, we believe that the most convenient approach to the irrigation control problem is, rather than looking for simplistic heuristics, to resort to a model-based control approach, where an observer is used to estimate the state of the entire orchard and a state-based feedback control law is used to track the desired reference.

In the next two sections we will report our preliminary analysis on the definition of observers and control laws for the problem at hand.

#### 3.2.2 Observers

As already said, the overall orchard can be seen as a system consisting of  $N$  plots and  $n$  plants, described by the following linear dynamical system:

$$\begin{aligned}\dot{\theta}_i &= -c_{1,i} * \theta_i + \sum_{k \in N_i} \eta_{k,i} (\theta_k - \theta_i) - c_{5,i} * ET_o(t) + \varphi_i * R_i(t) + \sum_{k \in U_i} \xi_{i,k} u_k, i = 1, \dots, N \\ \dot{W}_j &= \sum_{i \in V_i} c_{2,i,j} \theta_i(t) - c_{3,j} W_j(t) + c_{6,j} Et_o(t), j = 1, \dots, n \\ \dot{y}_{remote,j}(t) &= -\frac{2}{t_{delay}} y_{remote,j} + \left( \frac{2}{t_{delay}} + c_{3,j} \right) W_j(t) - \sum_{i \in V_i} c_{2,i,j} \theta_i(t) - c_{6,j} Et_o(t), j = 1, \dots, n\end{aligned}\quad (33)$$

For the sake of readability, let us rewrite this dynamical system in a matrix-based form as:

$$\begin{bmatrix} \dot{x}_1(t) \\ \dot{x}_2(t) \\ \dot{x}_3(t) \end{bmatrix} = \begin{bmatrix} A_{11} & 0 & 0 \\ A_{21} & A_{22} & 0 \\ -A_{21} & \frac{2}{t_{delay}} I_{n \times n} + A_{22} & -\frac{2}{t_{delay}} \end{bmatrix} \begin{bmatrix} x_1(t) \\ x_2(t) \\ x_3(t) \end{bmatrix} + \begin{bmatrix} B_1 \\ 0_{n \times m} \\ 0_{n \times m} \end{bmatrix} u(t) + \begin{bmatrix} B_{d1} \\ B_{d2} \\ -B_{d2} \end{bmatrix} Et_o(t) + \begin{bmatrix} \varphi \\ 0_n \\ 0_n \end{bmatrix} R(t) \quad (34)$$

where  $x_1 = [\theta_1, \dots, \theta_N]^T$ ,  $x_2 = [W, \dots, W_n]^T$ ,  $x_3 = [y_{remote,1}, \dots, y_{remote,n}]^T$ .

Notably, the dynamical system can be rewritten in a more compact form as:

$$\dot{x}(t) = Ax(t) + Bu(t) + B_{d,1}Et_o(t) + B_{d,2}R(t) \quad (35)$$

In particular, for what concerns the measurements, we will have continuous measurements from a set  $p < N$  soil moisture sensors and with no lack of generality let us assume that the measured parcels are the first  $p$ , so that the output is:

$$y_{moisture,i}(t) = e_i^T x(t), i = 1, \dots, p \quad (36)$$

Where  $e_i$  is the  $i$ -th vector of the canonical basis. In a vector form, the soil moistures measurements can be then denoted as:

$$y_{moisture}(t) = \Phi x(t) \quad (37)$$

where the matrix  $\Phi$  is defined as follows:

$$\Phi = \begin{bmatrix} I_{p \times p} & 0_{p \times (2n+N-p)} \\ 0_{(2n+N-p) \times p} & 0_{(2n+N-p) \times (2n+N-p)} \end{bmatrix} \quad (38)$$

Furthermore, for what concerns the data obtained by the remote sensing, all the plants will be sensed. Therefore, we can consider the following measurement vector:

$$y_{UAV}(t) = [0_{n \times N} \quad 0_{n \times n} \quad I_{n \times n}] x(t) \quad (39)$$

However, unlike the simple model we used in Section 3.1, it is not true that all the data are available at all time, but we have some of them only at some specific times (when the UAVs fly).

Accordingly, the output model we obtain is:

$$y(t) = \begin{bmatrix} I_{p \times p} & 0_{p \times \dim(\Gamma(t))} \\ 0_{\dim(\Gamma(t)) \times p} & \Gamma(t) \end{bmatrix} \begin{bmatrix} y_{moisture}(t) \\ y_{UAV}(t) \end{bmatrix} \quad (40)$$

where  $\Gamma(t)$  is a selection matrix that selects the data available at time  $t$ . Clearly this is a model with intermittent observations. As well known from the literature this kind of model it is easier to treat in discrete time. Accordingly, we will proceed to a sampling (with Zero Order Holder) of our plant and we will obtain a system in the form

$$\begin{aligned} x(t + T_s) &= A_{T_s}x(t) + B_{T_s}u(t) + B_d \begin{bmatrix} Et_o(t) \\ R(t) \end{bmatrix} \\ y(t) &= \begin{bmatrix} \Phi \\ [0_{p \times \dim(\Gamma(t))} \quad \Gamma(t)] \end{bmatrix} x(t) \end{aligned} \quad (41)$$

It should be noticed that in order to estimate the state for this kind of systems, we will use a modified version of the intermittent Kalman filter as proposed in [26], [27] the takes into account the presence of the matrix  $B_d$ .

### 3.2.3 Control of the entire orchard

For what concerns the control problem for a large-scale hazelnut orchard, several different control strategies can be conceived based on the availability of a state-observer, ranging from simple feedback control strategies to more complex and advanced control solutions.

Notably, before to focus on the control design problem itself, it should be noticed that the first problem to be addressed concerns the identification of a significant control objective. As already mentioned, ideally, we would like to reach a prescribed optimal quantity of water for each plant. However, due to the different way each plant reacts to water, this control objective could be only achieved if we were capable of controlling the inflow of water in each plant. Unfortunately, in the context of a real-world large-scale orchard this is not the case as the number of controllable valves  $p$  is usually much smaller than the number of plants  $n$ . Thus, it becomes clear that some realistic control criteria must be identified before to address the design control problem.

A possible way could be to define a cost function by considering a penalty term for not giving enough water to a certain plant, and a penalty term to account for the costs related to the waste of water. This cost function could be used both to define the prescribed reference (in the case of a traditional control law) or to define an optimal control problem.

Note that this cost function is in general case-dependent. For example, in the case of the field selected for the experimental validation within the “Azienda Agricola Vignola” where lines are well designed (i.e. the difference in water provided to each plant is small) and the cost of water is very low compared to the economic revenue of the orchard, it is reasonable to consider as a good cost function one that aims at maximizing the well-being of each plant.

Clearly, based on this control objective different control strategies could be defined. In the PANTHEON project we believe that the fundamental characteristics that the control strategy should possess are: i) simplicity and ii) scalability.

In this deliverable, based on these observations concerning the needs of our case study and by following the simplicity and scalability principles leading the research within the PANTHEON project, we propose a simple semi-decentralized control architecture. Note that, for the sake of simplicity and with no lack of generality, this control strategy is conceived under the assumption that each soil parcel has at most one plant on it, and that for each plant there is exactly one and only one water line (associated to one and only one water valve) giving directly water to it. In the case a plant should draw water from more than one parcel, we aggregate them (making a weighted average of the model variables). In this way we obtain  $n$  single soil parcel - single plant model which generalizes the control problem discussed in Section 3.1. In particular, we assume that each parcel has a virtual irrigation valve  $u_{virtual,j}, j = 1, \dots, n$ .

The control architecture we propose in this deliverable is as follows:

- 1) We control the  $n$  single soil parcel - single plant model independently and following the design proposed in Section 3.1, that is by determining the virtual command that should be actuated  $u_{virtual,i}, i = 1, \dots, n$
- 2) The actual actuated command is  $u_i = \max_{j \in T_{u_i}} \{u_{virtual,j}\}, i = 1, \dots, p$  where  $T_{u_i}$  is the set of trees “served” by the  $i$ -th real actuator.



The rationale of this control law is that the plant that needs water the most will be always the one that is served. As a matter of fact, the other trees might receive more water than needed, but this eventually, accordingly to the selected cost function, is acceptable, as far as there are no anomalies.

The main advantage of this approach is that it will be easy to tune and scale. Furthermore, it should be notice that no integral action is foreseen (and neither has been proposed in Section 3.1). The reason for this design choice is that in order to avoid strange behaviours, the integral gain should be so small that in order to be effective we would very likely be forced to manage it offline, that is changing it manually on the basis of historical data.

## 4 Validation of the model

The simulation model has been developed using [10] as a reference for the soil moisture and [21] for the plant model in terms of parameters. This intends to give reliability to the simulations done and the system developed for the control of the orchard.

In further tasks, these assumptions are going to be tested and validated using values from the orchard where different agronomic tests are going to be performed. In this validation part, some assumptions must be verified (absence of capillary rise or linear behaviour in the deep percolation) to obtain an accurate model where to perform and check different control strategies.

In these tests, we have established some protocols to be followed:

- High detail experimental soil mapping of experimental plots
- Plant response
- Water detection from the plant (Remote sensing)

Once the SCADA system is developed and more data and tools are available, more validation tests can be performed on site.

### 4.1 High detail soil mapping experimental plots

In precision agriculture, as we have shown, the knowledge of soil spatial variability is basic to understand the causes of crop variability and to correctly manage site-specific irrigation.

To obtain high detail maps of soil spatial variability, the research group of CREA, Research centre for Agriculture and Environment (CREA-AA, Florence) has developed a protocol. In this project, we would like to establish a collaboration with the CREA-AA centre to use this protocol in our experimental field and obtain a high detail soil mapping.

The protocol is elaborated as follows:

1. Survey with proximal soil sensors, namely electromagnetic induction sensor (EMI) and gamma-ray spectrometer. EMI sensor measures the apparent electrical conductivity at two different depths (about 0-75 cm and 0-150 cm), strongly correlated with soil texture, bedrock depth, moisture, salinity, stoniness, etc. Gamma ray spectrometer measure the spectra of gamma-rays, naturally emitted from the topsoil (about 0-30 cm). From the gamma-ray spectra, it is possible to calculate the total count of gamma-rays (TC), and the amount of the main radionuclides:  $^{40}\text{K}$ ,  $^{232}\text{Th}$ ,  $^{238}\text{U}$ . These data are related to the soil parent material mineralogy (volcanic rocks, limestone, etc.) and to the clay content, surficial stoniness, calcium carbonate, etc. The proximal survey allows to obtain very high detail maps (resolution: 0.5-1 m) of these parameters.
2. The maps obtained by proximal sensing and, eventually other maps obtained by the digital elevation model (slope, curvature, aspect) are used to delineate homogeneous areas and/or to decide the sampling sites, by method as k-means clustering.
3. The soils of the homogeneous areas are investigated by conventional pedological observation (augerings or trench profiles). The soil was described and sampling according the official international methods (FAO-IUSS-ISRIC). The soil samples are analyzed by standard laboratory analysis, to obtain: texture, pH, electroconductivity, total organic carbon, total nitrogen, calcium carbonate, cation exchange capacity and exchangeable bases.
4. Undisturbed soil samples can be collected to determine bulk density and water retention curves (water volume / tension). This allow to calculate soil available water capacity (AWC). Alternatively,



texture, bulk density, organic carbon and stoniness data allow to estimate AWC following several pedotransfer models, available in literature. Soil internal drainage can be measured on-site (Guelph permeameter) or estimated by pedotransfer models.

According to this protocol, it is possible to interpolate most of the soil variables through the whole field, by geostatistics (geographical regression, regression kriging, etc.), to obtain maps as: Soil available water capacity, soil depth, clay content, stoniness, etc.

47

Using this protocol, we could obtain a map of the different soil characteristics of the orchard and use this information for an accurate model of the water absorption depending on the area of the field.

#### 4.2 Leaf water test

The relative water content (%RWC) of a leaf is a measurement of its hydration status (actual water content) relative to its maximal water holding capacity at full turgidity. RWC test provides a measurement of the water deficit of the leaf and may indicate a degree of water stress in the plant.

The relative water content in different days and hours in the same day (RWC %) will be determined on the same trees adopting standardized procedure as:  $(FM - DM)/(TM - DM) \times 100$ , where FM is the fresh mass, DM the dry mass and TM the leaf mass after rehydration until saturation at 5 °C in the darkness.

The RWC% on hazelnuts have been validated performing a preliminary test with the field of the *Azienda Agricola Vignola* which have been selected for the experimental validation in order to observe the different values in irrigate and non-irrigated trees.

## References:

- [1] R. Romero, J. L. Muriel, I. García, and D. Muñoz de la Peña, "Research on automatic irrigation control: State of the art and recent results," *Agric. Water Manag.*, vol. 114, pp. 59–66, Nov. 2012.
- [2] C. Lozoya *et al.*, "Model Predictive Control for Closed-Loop Irrigation," *IFAC Proc. Vol.*, vol. 47, no. 3, pp. 4429–4434, 2014.
- [3] S. K. Saleem *et al.*, "Model Predictive Control for Real-Time Irrigation Scheduling," *IFAC Proc. Vol.*, vol. 46, no. 18, pp. 299–304, Aug. 2013.
- [4] C. Toureiro, R. Serralheiro, S. Shahidian, and A. Sousa, "Irrigation management with remote sensing: Evaluating irrigation requirement for maize under Mediterranean climate condition," *Agric. Water Manag.*, vol. 184, pp. 211–220, Apr. 2017.
- [5] K. Steppe, D. J. W. De Pauw, and R. Lemeur, "A step towards new irrigation scheduling strategies using plant-based measurements and mathematical modelling," *Irrig. Sci.*, vol. 26, no. 6, pp. 505–517, Sep. 2008.
- [6] L. G. Santesteban, S. F. Di Gennaro, A. Herrero-Langreo, C. Miranda, J. B. Royo, and A. Matese, "High-resolution UAV-based thermal imaging to estimate the instantaneous and seasonal variability of plant water status within a vineyard," *Agric. Water Manag.*, vol. 183, pp. 49–59, Mar. 2017.
- [7] M. Gerhards, G. Rock, M. Schlerf, and T. Udelhoven, "Water stress detection in potato plants using leaf temperature, emissivity, and reflectance," *Int. J. Appl. Earth Obs. Geoinformation*, vol. 53, pp. 27–39, Dec. 2016.
- [8] S. K. Ooi, I. Mareels, N. Cooley, G. Dunn, and G. Thoms, "A Systems Engineering Approach to Viticulture On-Farm Irrigation," *IFAC Proc. Vol.*, vol. 41, no. 2, pp. 9569–9574, 2008.
- [9] D. B. West, *Introduction to Graph Theory*, 2nd ed. Prentice Hall, 2000.
- [10] R. G. Allen, L. S. Pereira, D. Raes, and M. Smith, "Crop evapotranspiration - Guidelines for computing crop water requirements - FAO Irrigation and drainage paper 56," p. 15.
- [11] L. G. de Carvalho *et al.*, "FAO Penman-Monteith equation for reference evapotranspiration from missing data," *Idesia Arica*, vol. 31, no. 3, pp. 39–47, Oct. 2013.
- [12] J. Tous, J. Girona, and J. Tacias, "CULTURAL PRACTICES AND COSTS IN HAZELNUT PRODUCTION," in *Acta Horticulturae*, 1994, pp. 395–418.
- [13] J. G. PIQUERAS, "DEPARTAMENTO DE FÍSICA DE LA TIERRA Y TERMODINÁMICA," p. 331.
- [14] A. Cuesta, A. M. Jochum, and A. Cuesta, "TEC OLOGÍAS DE OBSERVACIÓ DE LA TIERRA E LOS SERVICIOS DE ASESORAMIE TO DE RIEGOS," p. 4.
- [15] E. G. Kullberg, K. C. DeJonge, and J. L. Chávez, "Evaluation of thermal remote sensing indices to estimate crop evapotranspiration coefficients," *Agric. Water Manag.*, vol. 179, pp. 64–73, Jan. 2017.
- [16] M. García Petillo and J. R. Castel, "Water balance and crop coefficient estimation of a citrus orchard in Uruguay," *Span. J. Agric. Res.*, vol. 5, no. 2, p. 232, Jun. 2007.
- [17] Y. De la Cruz, C. Martinez, and A. Pantoja, "Drip irrigation system based on distributed control — Part 1: Design and model," 2015, pp. 1–6.
- [18] K. Moore and Y. Chen, "Iterative Learning Control Approach to a Diffusion Control Problem in an Irrigation Application," 2006, pp. 1329–1334.
- [19] H. Verbeeck *et al.*, "Stored water use and transpiration in Scots pine: a modeling analysis with ANAFORE," *Tree Physiol.*, vol. 27, no. 12, pp. 1671–1685, Dec. 2007.
- [20] M. Bittelli, "Measuring Soil Water Content: A Review," p. 8, 2011.
- [21] K. Steppe, D. J. W. De Pauw, R. Lemeur, and P. A. Vanrolleghem, "A mathematical model linking tree sap flow dynamics to daily stem diameter fluctuations and radial stem growth," *Tree Physiol.*, vol. 26, no. 3, pp. 257–273, Mar. 2006.
- [22] Y. Cohen, V. Alchanatis, M. Meron, Y. Saranga, and J. Tsipris, "Estimation of leaf water potential by thermal imagery and spatial analysis\*," *J. Exp. Bot.*, vol. 56, no. 417, pp. 1843–1852, Jul. 2005.
- [23] V. Cristofori, R. Muleo, C. Bignami, and E. Rugini, "LONG TERM EVALUATION OF HAZELNUT RESPONSE TO DRIP IRRIGATION," *Acta Hortic.*, no. 1052, pp. 179–185, Sep. 2014.



- 
- [24] M. G. Bethune, B. Selle, and Q. J. Wang, "Understanding and predicting deep percolation under surface irrigation: UNDERSTANDING AND PREDICTING DEEP PERCOLATION," *Water Resour. Res.*, vol. 44, no. 12, Dec. 2008.
  - [25] R. L. Williams and D. A. Lawrence, *Linear State-Space Control Systems*. John Wiley & Sons, 2007.
  - [26] E. Garone, B. Sinopoli, A. Goldsmith, and A. Casavola, "LQG Control for MIMO Systems Over Multiple Erasure Channels With Perfect Acknowledgment," *IEEE Trans. Autom. Control*, vol. 57, no. 2, pp. 450–456, Feb. 2012.
  - [27] B. Sinopoli, L. Schenato, M. Franceschetti, K. Poolla, M. I. Jordan, and S. S. Sastry, "Kalman filtering with intermittent observations," *IEEE Trans. Autom. Control*, vol. 49, no. 9, pp. 1453–1464, Sep. 2004.